SGG SGS sc | nat
Swiss Journal of Geosciences

ORIGINAL PAPER Open Access

# Sedimentology of the Jura Molasse: Miocene tidal clastics and freshwater carbonates from the Tramelan-2 Borehole, NW Switzerland

Nigel H. Platt[1,2*] and Albert Matter[1]

**Abstract**

The Tramelan-2 borehole (Canton Bern, Switzerland) continuously cored a 275.60 m sequence of Palaeogene to Neogene sediments, providing a rare opportunity for sedimentological analysis of the Jura Molasse. Lithostratigraphy, sedimentary facies and heavy minerals allow correlation with the classical Swiss Molasse. Evidence for clastic input from Alpine and non-Alpine sources is consistent with deposition at the northern feather edge of the Molasse Basin. Grey sandstones at the base of the succession are tentatively interpreted as fluvial facies of the Lower Freshwater Molasse (USM). These are overlain by erosively-based conglomerates, interpreted as winnowed storm lags of locally-derived clasts and distantly-sourced Alpine material at the transgressive base of the Upper Marine Molasse (OMM). Above this, a range of plane-laminated and cross-bedded bioclastic sandstones are interpreted as the deposits of a meso- or macrotidal flat or estuarine complex. Facies evolution in the upper OMM records a series of stacked regressive cycles within an overall upward trend of reducing current energy, reflecting a transition from offshore to nearshore shallow marine environments. The unconformably overlying Upper Freshwater Molasse (OSM) passes upwards from micaceous siltstones and marls into a series of freshwater carbonates, dominated by lacustrine limestones which are arranged in repeated regressive cycles, each capped by organic-rich horizons. The middle part of the carbonate interval comprises palustrine limestones with pedogenetic fabrics recording periodic subaerial exposure. Stable isotope signatures from the palustrine facies reflect subaerial pedogenetic overprint, while the lacustrine carbonates record cyclical variations in $\delta^{13}C$ which may reflect increases in organic material during progressive lake fill and/or an increased influence of aquifer waters during flooding events. The Jura Molasse onlapped a Mesozoic carbonate pediment hosting a regional karst system which remained active at least until the Burdigalian transgression on footwall highs bounding the Delémont Basin, and locally into the Langhian near Tramelan. This configuration controlled subsequent deposition of OSM carbonates which onlapped erosional and potentially early tectonic relief, and were deposited in groundwater-fed seasonal lacustrine/palustrine environments, where the karstic aquifer controls on seasonal hydrology appear to have been comparable to Caribbean freshwater carbonate wetland systems today.

**Keywords** Jura, Swiss Molasse Basin, Miocene, Shallow marine clastics, Tidal deposits, Lacustrine/palustrine freshwater carbonates, Onlap, Karstic aquifer, Groundwater recharge

Editorial handling: Wilfried Winkler.

*Correspondence:
Nigel H. Platt
nigelplatt@yahoo.com
Full list of author information is available at the end of the article

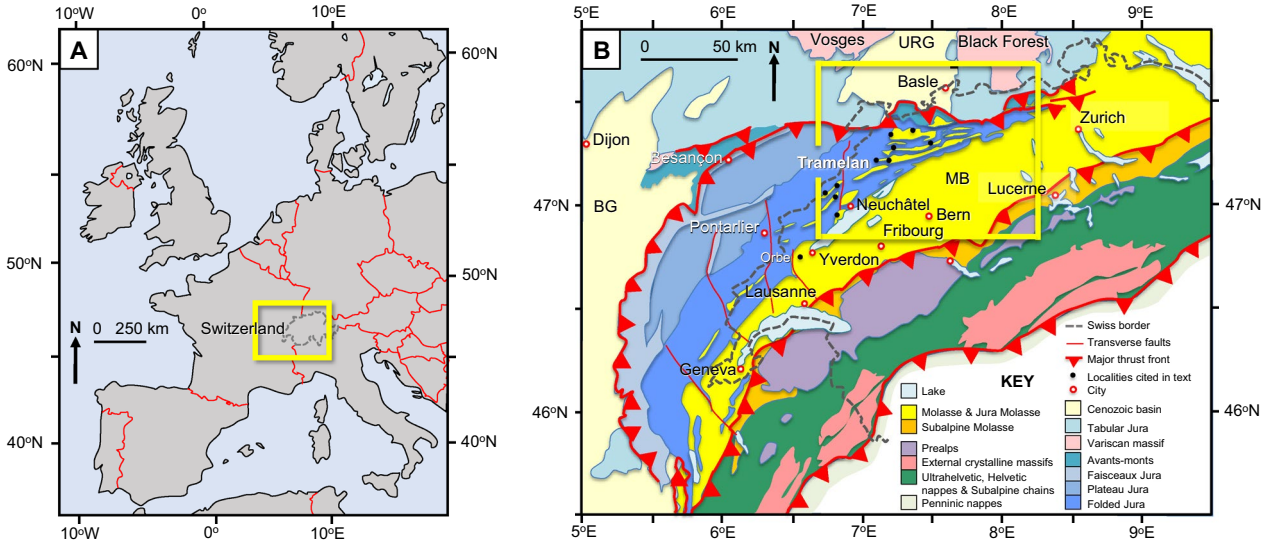


**Fig. 1** **a** Map showing location of Switzerland in central Europe. Yellow box shows area in **b**. **b** Geological map of the Swiss Alps and Jura, modified after Rime et al. (2019). MB: Molasse Basin. URG: Upper Rhine Graben; BG: Bresse Graben. Yellow box shows area in Fig. 2

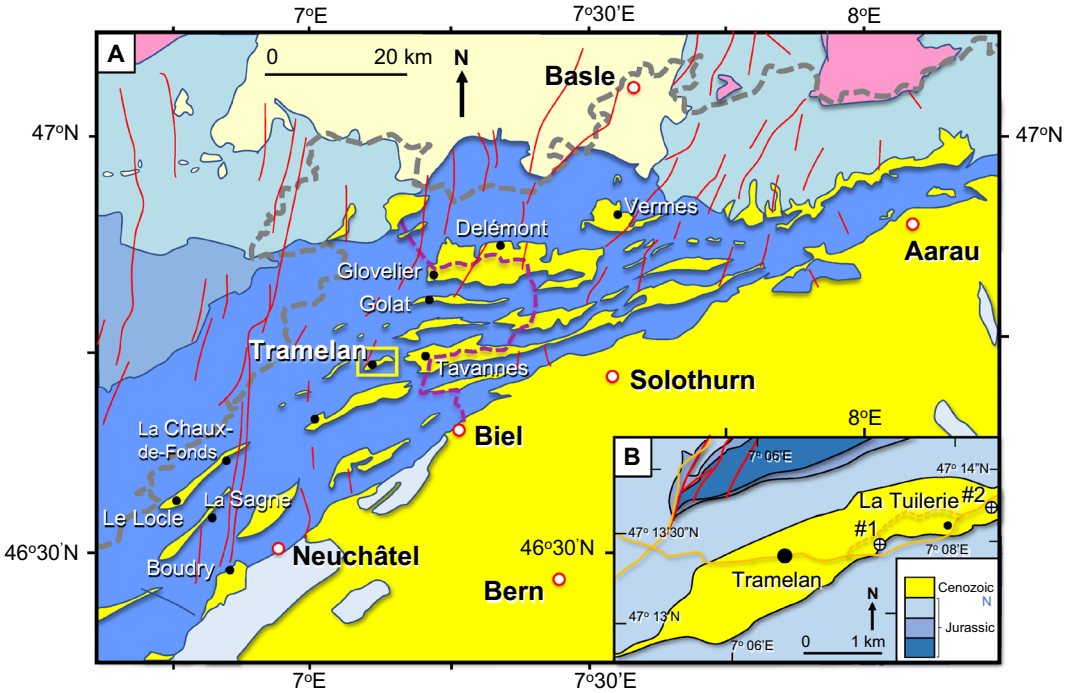


**Fig. 2** **a** Simplified geological map of NW Switzerland, simplified after Spicher (1980): Tektonische Karte der Schweiz (1: 500,000). Schweizerische Geologische Kommission. Yellow box shows area in **b**. Thick dashed grey line: national frontier. Thick dashed purple line: course of the A16 Trans-Jura motorway. **b** Geological map of the Tramelan syncline showing location of the Tramelan-1 and Tramelan-2 boreholes

## 1 Introduction

The Jura (Figs. 1 and 2) forms an arcuate range of folded and thrusted Mesozoic carbonates lying to the northwest of the Molasse Basin in Switzerland (Trümpy, 1980; Burkhard & Sommaruga, 1980), France and Germany. While the external sector of the Tabular Jura to the northwest is largely undeformed, the more internal Plateau Jura to the southeast is characterised by localised

areas of intense deformation in the Faisceau Jura (Chauve et al., 1980; Madritsch et al., 2008; Ziegler & Fraefel, 2009). By contrast, the structure of the Folded Jura of NW Switzerland (Laubscher, 1965, 1977, 1981, 1987, 1992; Schori et al., 2021) is defined by NE-SW trending anticlinal limestone ridges and intervening synclinal valleys where Cenozoic continental and marine sediments rest directly on the karstified Mesozoic surface. This region lies at the northern, former feather edge of the Molasse Basin (Heim, 1919; Homewood et al., 1986; Matter & Weidmann, 1992).

Evidence of clastic input from non-Alpine sources to the north led several authors to discuss the possibility that the Molasse Basin was at least intermittently connected with the Upper Rhine Graben (URG) via a NNE-SSW sedimentary conduit through the Jura area termed the "Rauracian Depression" (Baumberger, 1927; Reichenbacher et al., 1996; Berger et al., 2005b; Mojon et al., 2018). A degree of structural linkage between the two areas is implied by the continuation of N-S to NNE-SSW trending regional faults bordering the URG into the Delémont area of the Jura as shown in Fig. 2 (see also Roussé, 2006; Pirkenseer et al., 2018).

The Lower Freshwater Molasse (USM), Upper Marine Molasse (OMM) and Upper Freshwater Molasse (OMM) of the Jura provide a record of Palaeogene to Neogene deposition in the area between these important depocentres. The Oligocene and Miocene strata preserved in Jura synclines today appear to record complex and potentially distinct sedimentary histories with laterally variable facies which are challenging to correlate (Berger et al., 2005a, 2005b, 2011).

The Palaeogene to Neogene succession of the Molasse Basin is dominated by clastic rocks (Matter et al., 1980; Homewood et al., 1986; Keller, 1989; Kempf et al., 1999; Platt & Keller, 1992; Schlunegger et al., 1993, 1997a, 1997b) and thins northwards as it progressively onlaps a karstified pediment of Mesozoic carbonates in the Jura (Keller, 1992). There are significant stratigraphic gaps, for example in the Aquitanian which is absent in many areas of the Jura.

Carbonate intervals also occur in the Molasse at the northern margin of the Molasse Basin and in the Jura. The basal USM Lower Limestones are developed between Yverdon and Neuchâtel (Platt, 1992; Becker et al., 2001a, 2001b) while the USM Delémont Limestones occur in the central Jura (Picot et al., 1999). A younger series of freshwater carbonates referred to as the 'Oehningian' also occurs in the OSM (Kälin, 1993; Clement & Berger, 1999; Becker, 2003).

The areal distribution of the key lithostratigraphic units is shown in the excellent regional correlations and palaeogeographic maps presented by Berger et al., (2005a, 2005b) as also updated recently by Mojon et al. (2018) and Pirkenseer et al. (2018).

The drilling of the Tramelan-2 borehole in one of the synclines in the central Jura Mountains to a Total Depth of 275.60 m (Bertrand, 1990) permitted detailed study of the Molasse succession at this location. This paper presents sedimentological descriptions and interpretations of the clastic and carbonate units, with additional heavy mineral data and stable isotope results also collated from the clastics and carbonate rocks respectively. Together, these allow an assessment of the likely sediment sources active during deposition and provide important insights into basin evolution and palaeohydrology during Palaeogene to Neogene deposition in this area.

## 2 Material and methods

Drilling of the two Tramelan boreholes in the late summer and autumn of 1988 formed part of a hydrological study of groundwaters within an actively circulating karst system developed at the top of the Jurassic succession (Bertrand, 1990). A first borehole, located at the eastern edge of Tramelan village (co-ordinates 2575.980/1230.395) reached Mesozoic strata at a depth of only 5.75 m, subsequently penetrating a Marine Jurassic succession of Tithonian to Kimmeridgian age and reaching a Total Depth of 164.50 m. A second borehole was located 2 km to the east of Tramelan and south of the River Trame near La Tuilerie, at co-ordinates 2577.410/1230.935. Drilling penetrated a thick sequence of Palaeogene-Neogene Molasse sediments before reaching Total Depth in sandstones of the Lower Freshwater Molasse at 275.60 m.

Both boreholes acquired continuous 10 cm diameter cores. The core from the Tramelan-2 borehole was transferred to the Institut für Geologie at the Universität Bern for sedimentological logging, sampling for heavy minerals, micropalaeontological determinations and stable isotope analysis. Facies descriptions and stratigraphic analysis were carried out on 1 m core sections. Core photographs are included as supporting information (Additional File 1). 50 thin sections were made for microfacies analysis. Heavy mineral samples were taken every 5–10 m; the depths given refer to the first and last sample in each case.

160 samples of representative carbonate facies were selected for isotope analyses and taken from split core sections before being reacted in an on-line automated carbonate preparation system linked to a VG Prism II ratio mass spectrometer. Approximately 10 mg of powdered sample was reacted in "100%" $H_3PO_4$ for 10 min at 90 °C. Reproducibility of istotopic ratios of standard materials in the system was better than 0.1 ‰ for $\delta^{18}O$ and 0.05 ‰ for $\delta^{13}C$.

## 3 Geological setting and lithostratigraphy

The Tramelan syncline (Fig. 2) trends ENE-WSW, with northern and southern limbs exposing Upper Jurassic Kimmeridgian and Tithonian marine carbonates. Molasse sediments of Oligocene and Miocene age are present in the axis of the syncline (Aufranc et al., 2016a).

The established lithostratigraphy of the Jura was based on the work of Rollier (1892, 1893), who also carried out the original mapping (Rollier, 1898, 1900). Later studies permitting refinements and modifications of the lithostratigraphy were carried out by Frei (1925), Liniger (1925), Baumberger (1927), Rothpletz (1933), Forkert (1933), Schlaich (1934), Ziegler (1956), Antenen (1973) and Becker (2003) as summarised by Aufranc et al., (2016a, 2016b; 2017). The stratigraphy of the Upper Rhine Graben to the north was reviewed by Sissingh (1998).

The chronostratigraphy of the Molasse Basin to the south of the study area was established by Schlunegger (1997a), while the sedimentary evolution of the Molasse Basin was evaluated in detail by Keller (1992) and Strunck and Matter (2002). Important regional correlation studies were presented by Berger et al., (2005a, 2005b) and Berger (2011), drawing on the work of Picot (2002) and Becker (2003). Further syntheses were presented in relation to the Palaeogene by Mojon et al. (2018), with significant modifications and correlations with the URG also proposed by Pirkenseer et al. (2018). New data referring to the Neogene (Burdigalian) section in the Jura were provided by Prieto et al. (2018).

Lithostratigraphic schemes in the area are complex and feature nomenclature in two languages. Table 1 therefore provides a glossary of English and equivalent German and French stratigraphic units in common use. Figure 3 presents a simplified lithostratigraphy for the area in English, while Fig. 4 places the local succession in the

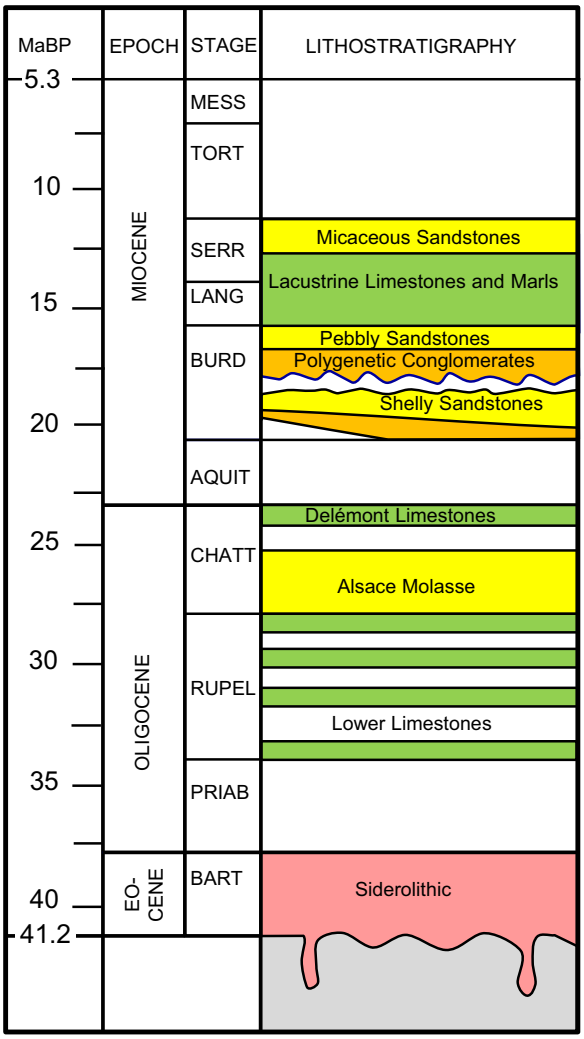


**Fig. 3** Generalised stratigraphy and facies of the Jura Molasse. Chronostratigraphic ages are from Cohen et al. (2022)

**Table 1** Summary chart of key stratigraphic units referred to in the text, together with their German and French language equivalents

| Age | Stage | | Unit | German | | Abbreviation & Fm | | French | |
|---|---|---|---|---|---|---|---|---|---|
| Miocene | Serravallian - Langhian | Upper Freshwater Molasse | Micaceous Sandstones | Obere Süsswassermolasse | Glimmersand | OSM | | Molasse d'eau douce supérieure | Grès micacé |
| | | | Freshwater Limestones and Marls | | Süsswasserkalke und –mergel | | | | Calcaires d'eau douce et marnes |
| | Burdigalian | Upper Marine Molasse | Pebbly Sandstones | Obere Meeresmolasse | Geröllsande | OMM | St.-Gallen Fm | Molasse marine supérieure | Sables à galets |
| | | | Polygenetic Conglomerates | | Polygene Nagelfluh | | | | Poudingue polygénique |
| | | | Shelly Sandstones / Grey Molasse | | Muschelsandstein / Graue Molasse | | Lucerne Fm | | Grès coquillier / Molasse grise |
| | Aquitanian | Lower Freshwater Molasse | ABSENT ? | | | | | | |
| Oligocene | Chattian | | Delémont Limestones | Untere Süsswassermolasse | Delsbergersüsswasserkalke | USM | | Molasse d'eau douce inférieure | Calcaires delémontiens |
| | | | Alsace Molasse | | Elsässer Molasse | | | | Molasse alsacienne |
| | Rupelian | | Lower Limestones | | Krustenkalke | | | | Calcaires inférieurs |
| | | Lower Marine Molasse | ABSENT ? | Untere Meeresmolasse | | UMM | | Molasse marine inférieure | |
| Eocene | Bartonian to Serravallian | | Siderolithic | | Siderolithikum | | | | Sidérolithique |
| Jurassic to Cretaceous | | | | | | | | | |

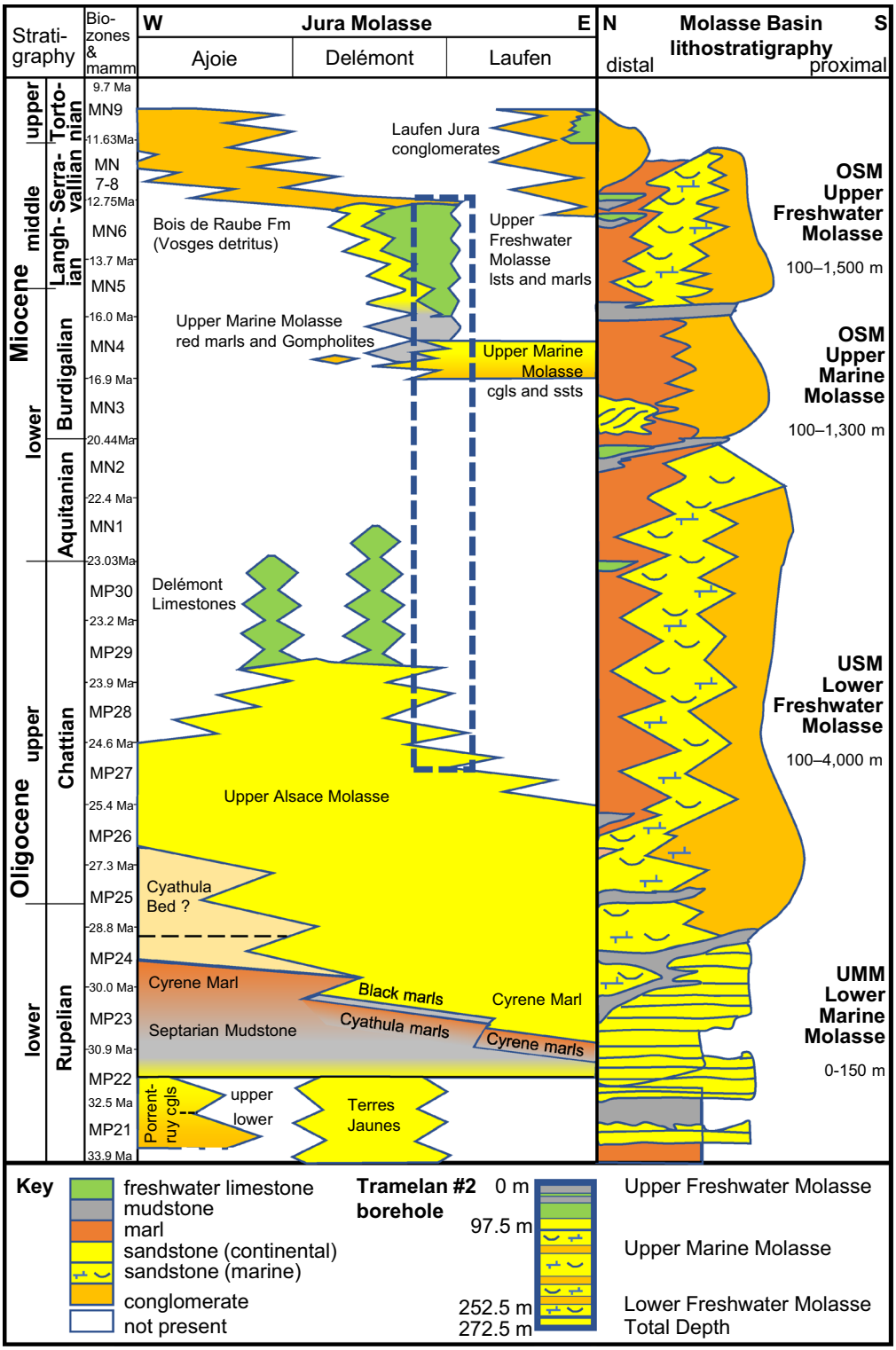


**Fig. 4** Generalised stratigraphy and facies of the Jura Molasse. The blue dashed rectangle illustrates the succession penetrated in the Tramelan-2 borehole. Adapted from unpublished figure courtesy of and with kind acknowledgment to Dr. Damien Becker (2022 unpublished data). Molasse Basin lithostratigraphy adapted after Keller (1992) and Sommaruga (1996). See Pirkenseer et al. (2018) for alternative stratigraphic synthesis and correlations with the URG. Chronostratigraphic ages are from Cohen et al. (2022)

context of an updated and more detailed summary of Palaeogene-Neogene stratigraphy in the Jura compiled by Becker (2022 unpublished data).

Throughout the Jura, a mineralised deposit known as the *Siderolithic*, including thin sandstones and gastropod limestones, rests on and is preserved in pockets within Mesozoic strata which form a regional karstified pediment (Baumberger, 1923; Rollier, 1910; Weidmann, 1984). The Siderolithic is generally assigned to the Eocene on the basis of mammal teeth finds and the Oligocene age of overlying deposits. However, Hofmann et al. (2017) postulated that the Siderolithic was a *terra rossa* deposit which continued to be formed until significantly later, with new dating from the northern and eastern Jura indicating that karstification and/or active karstic circulation continued or resumed during the Miocene up to c. 15 M yr BP.

The Siderolithic is unconformably overlain by the Palaeogene-Neogene succession, and appears to record a stratigraphic gap when Jurassic and Lower Cretaceous marine carbonates were subaerially exposed. The length of this stratigraphic gap is interpreted to increase northwards.

Thus on the northern margin of the Molasse Basin at the southern edge of the Jura, the Siderolithic is overlain by Oligocene fresh-water carbonates of the *Lower Limestones*. Further north (as in Tramelan-2), these strata may be missing and the karst surface appears to be overlain by sandstones of the *Alsace Molasse*, thinning to the northwest (Aufranc et al., 2016a) and marls and freshwater carbonates of the *Delémont Limestones*. These units form the Lower Freshwater Molasse (USM), which is present in the Tramelan-2 borehole and at La Tuilerie (Fig. 2) in the SE of the Tramelan syncline, but absent in Tramelan-1 (Bertrand, 1990) and in western areas of Tramelan village 1.5 km and 3.5 km to the west respectively (Aufranc et al., 2016a).

The unconformably overlying Upper Marine Molasse (OMM) of the Jura has four units (Becker, 2003; Zulliger, 2008; Aufranc et al., 2016b; Garefalakis & Schlunegger, 2019). The basal Burdigalian comprises grey sandstones of the *Grey Molasse* and the calcareous *Shelly Sandstones* (together the Lucerne Formation). The upper Burdigalian comprises coarse clastics of the *Polygenetic Conglomerates* and *Pebbly Sandstones* (making up the St-Gallen Formation).

In the southern Jura, these OMM deposits rest on variably truncated sections of the USM. However, at Glovelier, only 10 km NE of Tramelan-2, the USM is missing and the OMM succession rests directly on the karstified top Mesozoic surface, which includes karstic pockets with infill of Burdigalian age (Hug et al., 1997; Becker, 2003; Prieto et al., 2018).

The OMM is overlain by brackish to freshwater strata of the Langhian-Serravallian Upper Freshwater Molasse (OSM), comprising grey and black carbonates of the *Freshwater Limestones and Marls*, and green or grey marls and sandstones of the *Micaceous Sandstones*.

## 4 Borehole sequence and lithostratigraphic correlation

A simplified borehole log is shown in Fig. 5, with the main units described in the text below.

### 4.1 Grey sandstones (275–252 m)

The basal part of the succession comprises a series of 1 m bedded, dull grey-greenish medium-fine grained micaceous sandstones, locally cross-bedded with rare 30 cm thick coarse- to medium-grained graded grey sandstone units and intercalated 20 cm conglomerate horizons.

#### *4.1.1 Interpretation*

Sedimentological analysis of this interval is challenging. Neither marine indicators nor shale interbeds are present and these strata are interpreted as high energy braided stream deposits.

#### *4.1.2 Stratigraphic assignment*

The colours, lithology and abundance of muscovite are similar to those of the Alsace Molasse (Rollier, 1893), suggesting attribution to the USM. Further north in the URG, Roussé (2006) describes a sandy Lower Alsace Molasse containing shallow marine sedimentary structures, overlain by a continental fluviatile Upper Alsace Molasse which is potentially similar to the section in Tramelan-2. However, Antenen (1973) described the Alsace Molasse of the Jura as a series of sandstones interbedded with mottled overbank marls and paleosols similar to those developed in the Molasse Basin USM (c.f. Platt & Keller, 1992) but which are absent here.

The Alsace Molasse is overlain by marls and freshwater carbonates of the Delémont Limestones across much of the central and northern Jura, which were described by Kälin (1993, 2001) and Becker (2003) and dated as MP29-30 (Upper Chattian to basal Aquitanian). Thicknesses of the Délemont Limestones are variable, with construction of the A16 Transjura motorway near Tavannes 10 km to the east (Zulliger, 2008) revealing a section c. 5 m thick, overlain by a red sandy interval dated as MN2 (Aquitanian). The absence in Tramelan-2 of in situ Délemont Limestones and of this overlying Aquitanian section is consistent with localised truncation of the USM succession at an erosional unconformity below the base OMM.

An alternative interpretation could perhaps see the lowermost interval in Tramelan-2 as laterally equivalent to a significantly younger sandy Upper Marine

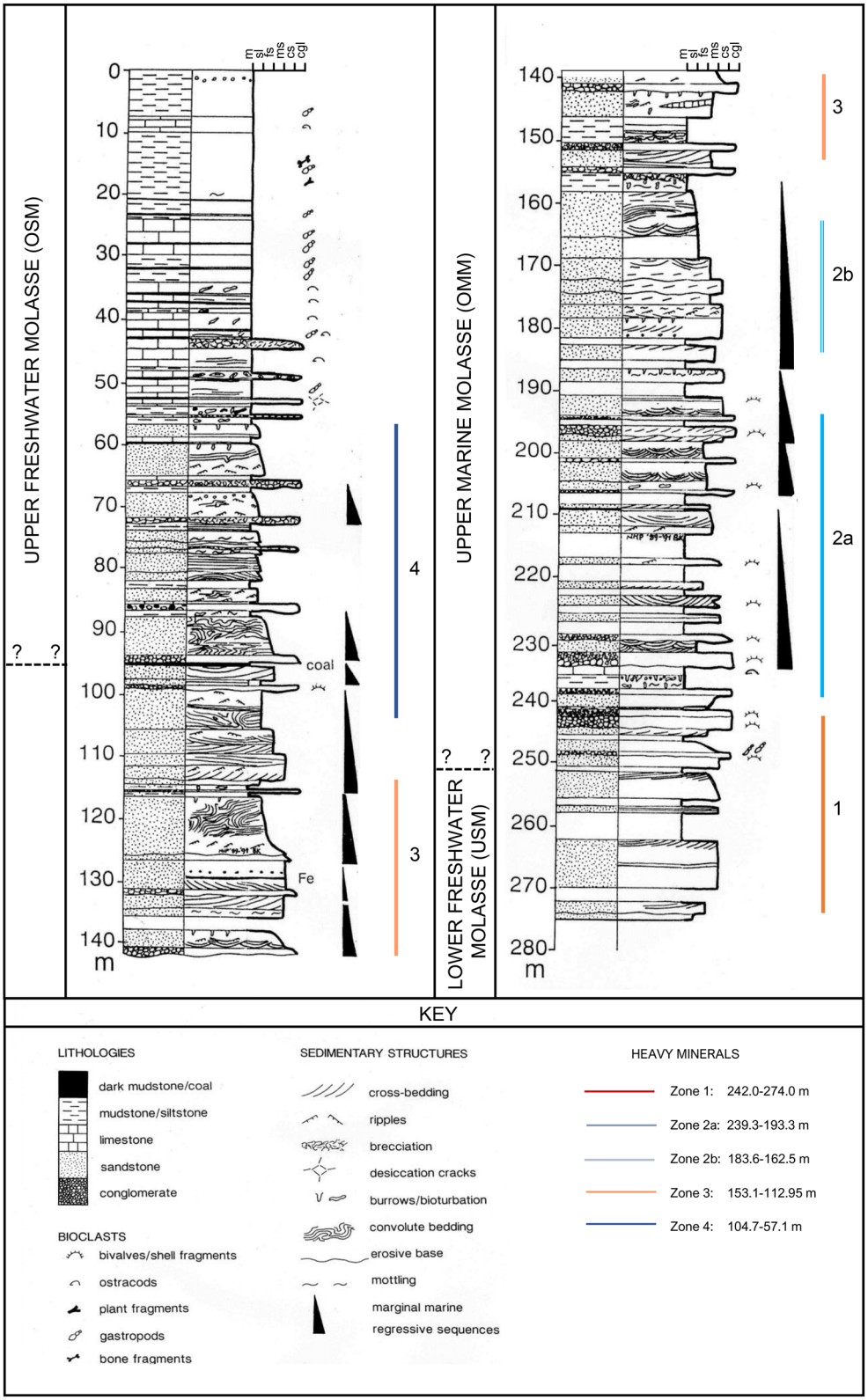


**Fig. 5** Borehole log showing lithostratigraphy and heavy mineral zones (see text discussion below)

Molasse sequence which overlies the Delémont Limestones in the adjacent Tavannes syncline and is assigned to mammal zone MN 2 (Late Aquitanian) by Zulliger (2008). In their Figure 3–13, Becker (2003) placed this series in Early Burdigalian zone MN3a, a unit of the Grey Molasse which forms part of the OMM and more typically displays marine sedimentary structures.

### 4.2 Green and grey sandstones and conglomerates (252–190 m)

A 35 cm thick conglomerate horizon at 249.25 m contains polymict clasts 2–5 cm across. This conglomerate is overlain by a thick alternation of polymict conglomerates and rippled or cross-bedded pale green or pale grey coarse sandstones. The sandstones have erosive bases, rare rippled layers and intercalated mudstone horizons. Interbedded coarser-grained layers up to 10 cm in thickness contain abundant 1–5 mm white bivalve fragments. Towards the top of the unit, the sandstones include reworked cm-scale sandstone chips. The presence of rip-up clasts, cross-bedding and ripple structures indicates a relatively high energy and shallow water environment.

The conglomerates contain clasts of quartzite, gneiss and limestone up to 10 cm in size. The conglomerate horizon at 235 m is underlain by a 1 m interval of white ostracodal limestone, which in turn rests on a 2 m thick grey-green mottled marl.

#### *4.2.1 Interpretation*

The varied clast sizes of the conglomerates and their sharply erosive bases are consistent with deposition in high energy events which reworked the underlying substrate while supplying pebbles from erosion in the catchment area.

Many of the pebbles are of Mesozoic carbonate and are probably locally derived, while the gneiss and quartzite pebbles were likely transported from more distant sources prior to deposition as winnowed storm lags. As described above, the context of the 1 m limestone interval at 236 m potentially suggests deposition as a large clast of reworked Delémont Limestone.

The poor sorting of the coarser sandstones and their sedimentary structures indicate deposition by high energy currents as may occur in tidal channels and bars (de Raaf & Boersma, 2007). Rapid migration of tidal channels is likely to have favoured preservation of the channel facies while the sediments of topographically higher bars and sand flats were preferentially eroded.

The medium- to coarser grained units show low angle cross-bedding and numerous reworked sandstone and/or mudstone clasts. Their poor sorting suggests variable current energy, and low angle cross-bedding is consistent with lateral migration of large scale sedimentary structures; similar deposits were interpreted by Keller (1990) as point bar deposits of large tidal channels.

#### *4.2.2 Stratigraphic assignment*

Garefalakis and Schlunegger (2019) inferred northward onlap of a basal OMM1 section of lower Burdigalian MN3a age in northern areas of the Molasse Basin bordering the Jura to the SW of Tramelan near Lake Neuchâtel (see Fig. 2). This interpretation is consistent with an MN3a age determination for the basal OMM in the Tavannes syncline obtained by Beaumont et al. (1984).

In the northern axis of the Molasse Basin, Garefalakis and Schlunegger (2019) assigned an MN3b age to the Shelly Sandstones. This unit contains abundant molluscan shell fragments (Allen et al., 1985) and in many areas east of the Napf Fan also contains debris of the echinid *Scutella* sp., while further west comprising sandy pelecypod-bearing packstones with barnacle fragments.

The interbedded and overlying polymict conglomerates are typically assigned to the Polygenetic Conglomerates. Elsewhere in the Jura, as here, this unit commonly includes reworked clasts of Delémont Limestone as well as of Shelly Sandstone (Antenen, 1973).

According to Antenen (1973), the Shelly Sandstones and Polygenetic Conglomerates are rarely found together. Conglomeratic intervals have historically been attributed to the "Helvetian", an informal local stratigraphic name used for conglomerate-bearing facies (see discussion in Becker, 2003), with a later Burdigalian age inferred on the basis that the conglomerates must be somewhat younger than the sandstone units from which some of their clasts were derived.

In the Tramelan-2 borehole, conglomerate and shelly sandstone facies appear interbedded. In the absence of biostratigraphic control, an alternative interpretation could thus be considered that sedimentation reflected successive erosion and reworking during the Burdigalian transgression. In this interpretation, the Shelly Sandstones and Polygenetic Conglomerates would represent regionally persistent and diachronous sedimentary facies laid down during episodic sea level rise (Figs. 2 and 3; discussion in Naef et al., 1985). Conglomerates would then represent the initial transgressive deposits in each case, overlain by Shelly Sandstones, before the deposition of further conglomerate horizons containing reworked Shelly Sandstone clasts.

A similar contact between the USM and the overlying OMM Lucerne Formation was exposed by the A16 motorway in the Tavannes syncline 5 km to the east (Mojon et al., 2018). A 2 m thick basal lag of sandy

conglomerate at that locality featured pebbles of probable Alpine origin, as well as shark teeth, bivalves, bryozoans and well-rounded mammalian bones and reworked caliche nodules. This initial transgressive lag was then overlain by bioclastic sandstones assigned to the Shelly Sandstones by Zulliger (2008).

Similarly, Aufranc et al. (2016b) describe a polymict conglomerate of quartzite, granitic and limestone clasts resting on the Delémont Limestone at La Tuilerie near Tramelan. Although no detailed analysis was reported, this assemblage may reflect mixed source areas, with quartzite likely to have been derived from the Napf Fan to the south while porphyrite and Triassic Buntsandstein clasts seen further north in the Delémont Basin point to source from the Vosges.

### 4.3 Pale beige and grey sandstones (190–95 m)

The grey and green Shelly Sandstones and Polygenetic Conglomerates are overlain by a thick series of sandstones containing rare carbonate pebbles. Pale beige deposits dominate from 190 to 169 m and from 142 to 127 m with mid-grey rocks between and above.

The lower part of this interval comprises fine-laminated muddy sandstone–siltstone–mudstone alternations with a wide variety of sedimentary structures including abundant current ripples, small-scale load structures and grading as well as lenticular, flaser and convolute bedding. Molluscan shell fragments are common in the coarse sandstone units of flaser sets.

These facies are overlain by a series of more massive sandstones above. Two thin limestone conglomerate horizons at 154.8 m and at 142 m contain sub-rounded beige, grey and brown carbonate clasts from 2 to 10 cm in size. The lower of the two horizons is 80 cm thick and rests on a heavily mottled grey marl horizon, while the upper one is 20 cm thick.

#### *4.3.1 Interpretation*

The range of sedimentary structures in coarser units indicates deposition by unidirectional currents of moderate velocity (> 0.45 $ms^{-1}$), while sandstone–siltstone beds are interpreted as suspension- and bed-load deposits (Reineck & Singh, 1980). The preservation of intercalated mudstone layers records deposition at intervening slack water phases. Variable current régimes are characteristic of tidal settings (Klein, 1975a; 1975b; Longhitano et al., 2012) with relatively low current velocities being typical of the upper zones of muddy tidal flats and salt marshes.

Rapid sedimentation leads to instability of saturated sediments and the formation of convolute and deformed bedding via dewatering. A rotated block of laminated fine sandstone at 105 m is interpreted as tidal flat material reworked via the erosional collapse of a tidal channel margin.

The green-grey fine muddy sandstones and marls which follow contain burrows and cm-scale brown or grey-green mottling but display few primary sedimentary structures. Their massive and homogeneous character is thought to reflect destratification through extensive bioturbation and root action from a well-developed terrestrial vegetation cover during emergence. These deposits are interpreted as being deposited in the marshy, supralittoral zones of a coastal tidal flat.

#### *4.3.2 Stratigraphic assignment*

The series of beige and grey sandstones in Tramelan-2 is assigned to the Pebbly Sandstones, part of the OMM. Comparison with Antenen's (1973) lithostratigraphy suggests that intercalated thin conglomerate horizons at 154.8 m and 142 m correspond to the Vêlé Limestone Conglomerate.

In the Molasse Basin, Garefalakis and Schlunegger (2019) described offshore deposits of the Shelly Sandstones as overlain by an upper OMM2 (St.-Gallen Formation) unit of likely MN4 age (Jost et al., 2016) comprising nearshore deposits of the *Coarse Sandstone* (Grobsandstein).

### 4.4 Siltstones, limestones and Marls (95–5 m)

A thin coal at 95 m is overlain by a series of green and grey-brown marls, locally containing reworked 1–10 mm angular clasts of limestone and organic-rich mudstone, with abundant gastropods and intercalated 1–2 m pale beige limestone horizons. Marls dominate up to 65 m, with limestones increasing above this and forming the entire sequence from 55 to 34 m.

The overlying interval from 34 to 5 m comprises grey-brown marls with abundant gastropods and interbedded 1–2 cm pale beige limestone horizons. Palaeontological determinations on samples from 32.4 to 10 m are presented in Table 2.

The intervals from 65 to 55 m and 45–34 m are arranged in decimetre- to metre-scale asymmetric cycles, commencing with sharp-based pale beige, laminated ostracod packstones and passing gradationally up into mid- and darker grey intraclastic or charophyte wackestone capped by cm-scale dark grey to black organic-rich or coaly horizons. This succession is interrupted from 55 to 45 m by a series of white brecciated limestones with pedogenetic fabrics.

Similar cycles are found at outcrop nearby (Fig. 6; see also Aufranc et al., 2016b). The cycles begin with pale grey carbonate, darkening upward towards dark grey,

**Table 2** Palaeontological determinations from the Upper Freshwater Molasse (kind courtesy of the late Prof. J.–P. Berger)

| Depth | Find | Remarks |
|---|---|---|
| 10.93 m | Many fish otoliths | |
| | 1–2 pharyngeal teeth | |
| | Abundant molluscs | Planorbids |
| | Rare ostracods | |
| | Charophytes | *Lychnothamnus* sp.<br>*Chara* sp. |
| 15.79 m | Abundant gastropods | Lymnaeids and Planorbids |
| | Fish otoliths | |
| | 1–2 pharyngeal teeth | |
| | Charophytes | *Lychnothamnus* sp. |
| | Mammal tooth | *Pseudodryomus* sp.<br>(B. Engesser det.) |
| 20.42 m | 2–3 otoliths and a few molluscs | |
| 21.37 m | 2 fish otoliths | |
| | 1 bone fragment | |
| | Mollusc fragments | |
| 26.28 m | Gastropod fragments | Helicids, Planorbids, Lymnaeids |
| | Gastropod opercula | |
| 28.40 m | Abundant molluscs | Planorbids, Lymnaeids |
| | 1–2 otoliths | |
| | 1–2 badly preserved charophytes | Probably *Chara* sp. |
| 28.62 m | Abundant fossil fragments | Lymnaeids, Planorbids, gastropod opercula |
| | 1 fish tooth | |
| | Charophytes | Indet. |
| 28.78 m | Molluscs | Planorbids, rare Lymnaeids |
| 30.10 m | Molluscs | Planorbids, rare Helicids and opercula |
| | 1–2 bone fragments | |
| | Charophyte | *Lychnothamnus* sp. |
| | 1? fish otolith | |
| 31.90 m | Rare gastropod fragments | Planorbids and Lymnaeids |
| 32.40 m | Abundant molluscs | Planorbids, Lymnaeids etc |
| | 1 pharyngeal tooth | |
| | 2 otoliths | |

*Lychnothamnus*—Miocene age; known throughout the Upper Freshwater Molasse

Palaeoecology—lacustrine/palustrine environment, probably freshwater. No brackish indicators

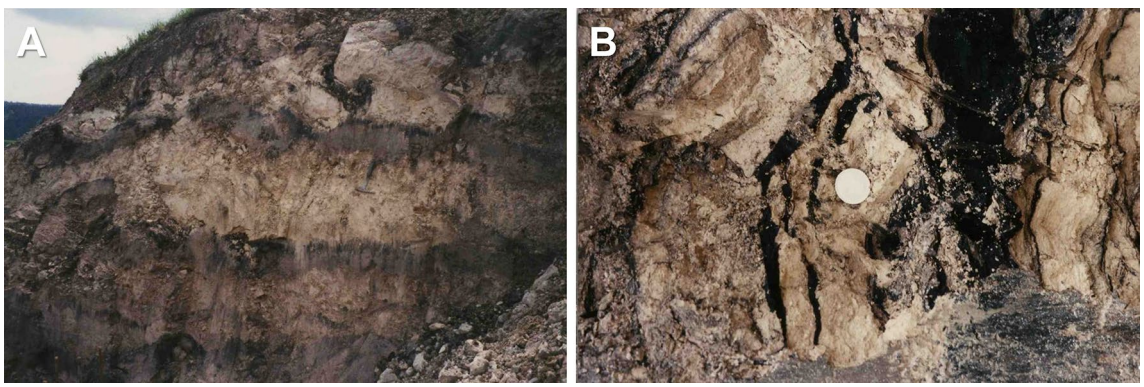


**Fig. 6** Outcrops near the Tramelan-2 borehole site, showing sedimentary cycles from light to dark lacustrine carbonates. **a** Vertical section, younging to top. **b** Detail showing weakly laminated limestone units capped by cm-scale sapropelic horizons (stratigraphic younging to the left)

organic-rich limestones. Rarer cm-scale sapropelic coal horizons are preserved beneath sharp and well-defined cycle tops.

Thin sections from the Tramelan-2 borehole reveal a variety of microfacies (Fig. 7):

1) Pale to mid-grey micritic limestones, with abundant gastropod and ostracod fragments (Fig. 7A), charophyte stems and gyrogonites and micritic limestone intraclasts (Fig. 7B) These limestones locally contain abundant spar-filled tubes 0.1 mm in diameter and up to 0.5 mm long (Fig. 7B and C).
   *Interpretation*
   The open, clotted fabric of this facies (Fig. 7B and C) is consistent with algal carbonate production while the sparry tubes appear similar to green algae described in Miocene lacustrine bioherms from the margins of the Ries Crater in Germany by Riding (1979). The absence of lamination suggests deposition in shallow, unstratified carbonate lakes.
2) White to pale grey strongly brecciated limestones, with angular 2–10 cm intraclasts of green marl and grey limestone, glaebules and circumgranular cracks (Fig. 7D).
   *Interpretation*
   Fabrics typical of pedogenetic brecciation and desiccation (Alonso Zarza, 2003) favour an interpretation as palustrine carbonates modified during seasonal subaerial exposure.
3) Darker grey carbonates with abundant gastropods and a higher content of organic matter (Fig. 7E). Detrital quartz grains are locally abundant. Some limestones (e.g. at 45.4 m) show abundant angular cm-scale intraclasts.
   *Interpretation*
   The presence of intraclasts and detrital quartz indicates clastic influx and reworking. These carbonates are interpreted as organic-rich limestones ("gyttjas"; Stankevica et al., 2016) deposited in shallower water at a vegetated lake margin.
4) Homogeneous green marls with gastropod shells show only local weak lamination.
   *Interpretation*
   Lower carbonate contents suggests that these rocks were laid down during the early stages of freshwater deposition when clastic influx initially diluted carbonate production.

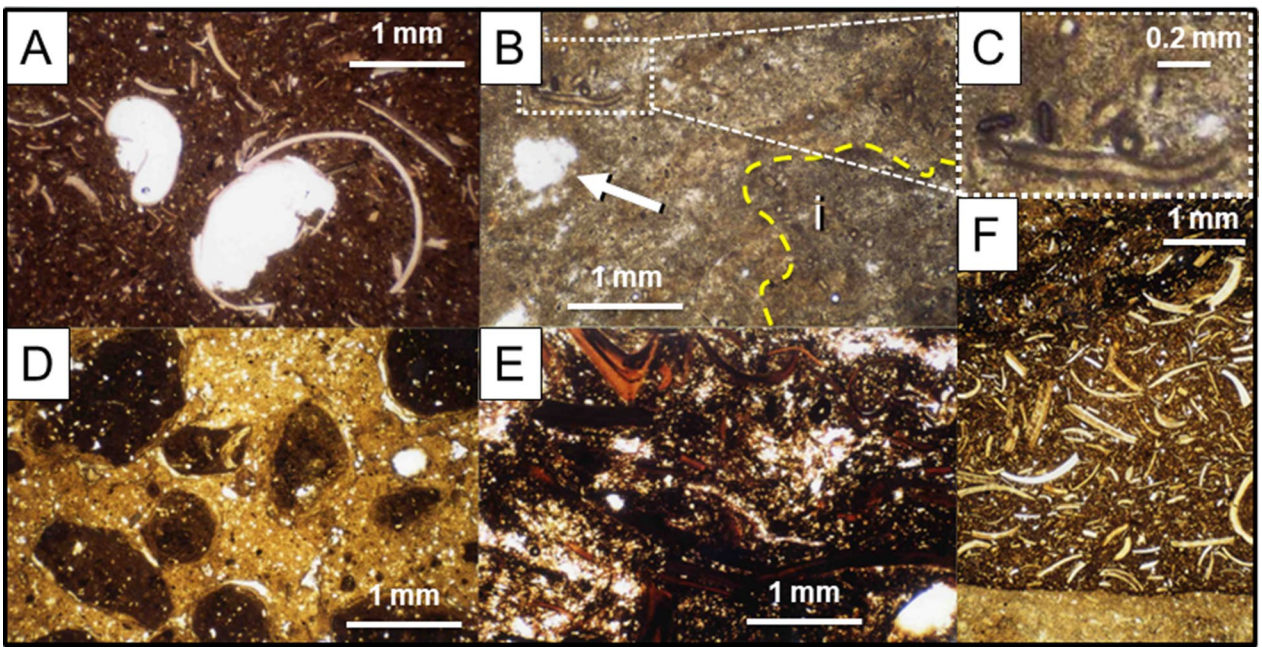


**Fig. 7** Thin section micrographs from carbonates in the Upper Freshwater Molasse. **a** Ostracod wackestone, **b** Clotted algal micrite with intraclast (i; yellow dashed outline), charophyte stem (arrowed) and area of detail shown in **c**. **c** Detail of image **b**, showing green algal filaments in longitudinal and cross sections. **d** Peloidal wackestone with circumgranular cracking, **e** weakly laminated organic rich limestone with shell fragments, **f** micritic mudstone overlain sharply by darker shelly wackestone with abundant gastropod shell fragments, grading up into organic rich mudstone

5) Light brown to beige laminated gastropod biomicrites. This rare facies shows weak mm-scale lamination and abundant gastropod shell fragments (Fig. 7F).
*Interpretation*
The preservation of weak lamination suggests limited bioturbation, consistent with deposition below a dysoxic water column, possibly in slightly deeper water.

#### *4.4.1 Discussion*

The varied facies of this limestone succession are interpreted as recording deposition in freshwater carbonate wetland environments characterised by limited fine clastic input, the accumulation of organic matter and colonisation by terrestrial snails.

A sharp-based basal limestone conglomerate horizon at 87 m may record initial flooding. The overlying strata from 86 to 65 m comprising green and brown marls, laminated siltstones and intercalated 50 cm thick limestone beds are interpreted as early phase ephemeral pond deposits.

These marls pass up into a series of stacked regressive cycles, each commencing with green lacustrine marls, overlain by open lacustrine ostracod packstones and algal wackestones and organic-rich marly-peaty horizons with abundant terrestrial snails. As noted above, these darker units are typically described as *gyttjas* (Stankevica et al., 2016), humic deposits which are rich in detrital organic matter and capped by cm-scale sapropelic coals (see Fig. 6). Similar facies are found in the Middle Miocene of the Steinheim Basin in SW Germany (Tütken et al., 2006).

Analogous facies occur in many modern temperate marl lakes of North America, with examples including Green Lake, New York (Dean & Fouch, 1983), and Lake Littlefield and Sucker Lake, Michigan (Murphy & Wilkinson, 1980; Treese & Wilkinson, 1982; Dustin et al., 1986). In these lakes, cyclical carbonates recorded successive periods of increased organic productivity and progressive shallowing resulting from sedimentary infilling (Platt & Wright, 1991). An ancient, large-scale analogue may be provided by the Lower Cretaceous Peterson Limestone of Wyoming and Idaho, which covers 20,000 km$^2$ and is up to 60 m thick (Glass & Wilkinson, 1980).

The brecciated palustrine limestones from 55 to 45 m clearly record periodic subaerial exposure, pointing to deposition in freshwater algal marsh environments subject to seasonal or longer periods of emergence (Platt, 1989; Alonso Zarza, 2003) and similar to those found in modern Caribbean coastal wetlands such as the Florida Everglades (Platt & Wright, 1992).

The influence of groundwater recharge on shallow palustrine-lacustrine systems was postulated by Wright and Platt (1995). Carbonate wetlands both in Florida and the Yucatán Peninsula of Mexico (Platt & Wright, 2019, 2023) overlie extensive regional carbonate pediments and are fed by underlying karst aquifer systems which control seasonal fluctuation of water levels. Regional karst systems also underlie extensive palustrine and lacustrine carbonates in the Early Cretaceous and the Palaeogene

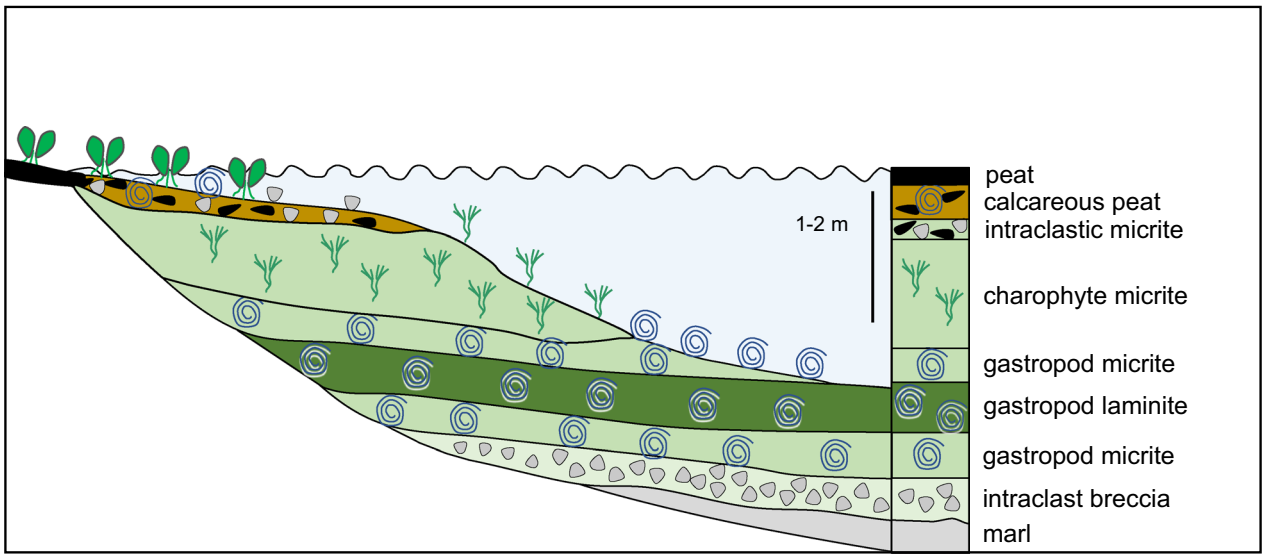


**Fig. 8** Facies model for Upper Freshwater Molasse carbonates in the Tramelan-2 borehole

of Iberia and NW Europe (Platt, 1989; Armenteros et al., 1997; Mas et al., 2019) which may rest either directly on a karstified carbonate pediment (Azêredo et al., 2015) or upon clastic successions which infill tectonically-created relief above it (Platt, 1995; Platt & Wright, 2023).

A range of continental facies and environments were recognised in the OSM by Kuhlemann and Kempf (2002), passing from alluvial fans in the south to more distal fluvial and lacustrine environments in northern areas of the Molasse Basin and the Jura. Becker (2003) proposed palaeogeographic models showing onlap of OSM deposits onto the marine Jurassic. We now interpret these OSM strata as recording seasonal subaerial exposure and pedogenetic modification of freshwater carbonates in response to variations in aquifer level in the underlying karstified Mesozoic carbonate pediment and its overlying clastic cover.

Figure 8 provides an integrated facies model for the OSM carbonates in Tramelan-2, drawing on similarities with the marl-peat cycles of the Michigan lakes described by Murphy and Wilkinson (1980) and Treese and Wilkinson (1982). Although modest cycle thicknesses of only 0.5 to 1 m may partly reflect compaction, they are consistent with formation in very shallow water bodies. The occurrence of organic-rich and rare laminated horizons is interpreted as reflecting episodic overproductivity resulting in intervals of dysoxia at the lake floor.

#### *4.4.2 Stratigraphic assignment*

A dark grey to black sapropelic coal at 95 m is interpreted as the base of the OSM, resting on the OMM below. This is overlain by a sandstone conglomerate and then by medium- to fine-grained sandstones. A limestone conglomerate at 87 m marks the sharp base of a carbonate succession in Tramelan-2 which appears to show a facies evolution similar to 'Oehningian' carbonates described from near La Chaux-de-Fonds and Le Locle, some 30 km to the southwest (Becker, 2003; Eichenberger et al., 2020). Mojon et al. (2018) recognised three lithological units in that area:

- A lower and marly Unit 1, transitional with the marine Burdigalian, locally displays a red colour ascribed to reworking of the Siderolithic (Kübler, 1962) and dated as MN4;
- The overlying 'Lower Oehningian' Unit 2 consists of fine grained, highly fossiliferous freshwater carbonates and marls and is dated as spanning zones MN5, 6 and 7–8;
- Finally an 'Upper Oehningian' Unit 3 contains dark organic-rich horizons near the top.

Kälin and Kempf (2009) recognised thirteen characteristic local mammal assemblages within the OSM distribution across the North Alpine Foreland Basin from SW France, through Switzerland and into Southern Germany. These assemblages span the European Neogene mammal (MN) units from MN4 to the base of MN9 (ca. 17.5–11 Ma), noting that further east in Southern Germany, Reichenbacher et al. (2013) recognised a transitional 'Upper Brackish Molasse' (OBM) of MN4a age between the OMM and OSM, with the base of the OSM placed at 16.6 Ma BP in that area and somewhat later at 16.0 Ma BP in the Swiss Molasse Basin, and noting also that the basal contact of the OSM may be erosive in both areas.

Biostratigraphic data from the Le Locle area to the SW of Tramelan-2 point to OSM carbonate sedimentation within a well-constrained interval in the Langhian–Serravallian from 14.0 to 13.5 Ma BP (Mojon et al., 2018). However, the basal unit (MN4) at La Chaux-de-Fonds/Le Locle and Tramelan-2 appears to be absent in the Jura synclines of La Sagne, Les Ponts-de-Martel, Vermes and Golat (see Fig. 2) where the oldest Oehningian strata are dated as MN5 (Kälin, 1993; Kälin & Kempf, 2009). This mild diachroneity was interpreted as a reflection of early Jura tectonics by Kälin et al. (2001), while Mojon et al. (2018) interpreted units 2–3 as recording the rich ecosystem of a large carbonate lake formed in a developing syncline surrounded by karstic topography. Freshwater carbonate deposition may thus have initiated in small and potentially isolated basins before expanding via onlap and overstep across a wider area.

The OSM succession at Tramelan-2 appears to show a broadly similar evolution of facies to that around Le Locle, in commencing with marls and passing through palustrine and lacustrine carbonates into cyclic alternations of organic-rich carbonate facies above, within which a grey-black marl with gastropod fragments at 21.3 m was dated from MN7 + 8 (Kälin, 1993). These correlations suggest that OSM environments and facies evolved in parallel across the area, either via direct connection, or via a common groundwater level which served to control water bodies which were intermittently isolated in structural compartments within the Jura at this time.

## 5 Stable isotope analyses

### 5.1 Isotopic data

Carbon and oxygen stable isotope data for 160 samples are presented on a cross-plot in Fig. 9A and versus depth in the core in Fig. 9B.

The pedogenetically modified carbonates from 57 to 45 m show only modest vertical variation in isotopic composition, displaying a narrow range in $\delta^{13}C$ from −6 to −4 ‰ PDB and in $\delta^{18}O$ from −4 to −1 ‰ PDB, while

over much of this interval $\delta^{13}C$ and $\delta^{18}O$ remain fairly constant at −5 and −2 ‰ respectively. A subset of samples with the lowest $\delta^{13}C$ values appears to show a degree of co-variance between $\delta^{13}C$ and $\delta^{18}O$ as shown by the trend line in Fig. 9A.

The lacustrine sediments show a wider range in stable isotope ratios, with cyclical variations of up to 4 to 5 ‰ in $\delta^{18}O$ and up to 6 ‰ in $\delta^{13}C$ carbon across intervals 50 to 100 cm thick. Carbon and oxygen isotopic ratios track broadly in parallel within several individual cycles (e.g. between 36–35 m and 44–42 m; Figs. 9B and 10), with more negative (lighter) isotopic ratios in darker facies of cycle tops and with abrupt positive shifts occurring at cycle boundaries.

### 5.2 Discussion

The stable isotope compositions of non-marine carbonates have been discussed in several major review papers including those by Kelts and Talbot (1990) and de Boever et al. (2017).

The isotopically-light carbon and isotope oxygen compositions and suggestions of partial co-linearity shown by the pedogenetic facies suggest deposition in closed hydrological settings with long residence times (Talbot, 1990). Similar stable isotopic values and trends are reported from palustrine and pedogenetic successions in the Upper Jurassic of the western USA (Dunagan & Turner, 2004), the Berriasian of Northern Spain (Platt, 1989), the Eocene of the Swiss Molasse Basin (Platt, 1992) and the Miocene of central Spain (Bustillo & Alonso Zarza, 2007) and are consistent with the incorporation of atmospheric $CO_2$ within pedogenetically overprinted carbonate modified during subaerial exposure (Cerling, 1984, 1991; Cerling et al., 1989).

Within the current dataset, the subset of samples from the palustrine facies appearing to show colinearity in Fig. 9 may reflect greater desiccation during subaerial exposure and pedogenesis, with colinearity reflecting evaporative effects on $\delta^{13}C$ and $\delta^{18}O$. The remaining palustrine samples with $\delta^{13}C$ and $\delta^{18}O$ values which are more similar to the lacustrine samples may reflect lesser subaerial exposure and/or bioturbational mixing in more hydrologically open conditions.

More negative $\delta^{13}C$ values in the palustrine carbonates may also record increased oxidation of organic material in seasonally flooded and subaerially exposed settings. Pederson et al. (2019) linked repeated wetting and drying with the delivery of isotopically light $^{13}C$ to the dissolved inorganic carbonate (DIC) pool from which the freshwater carbonates of the Florida Everglades were precipitated. Similar stable isotope compositions within parts of the Clino core drilled on the Great Bahama Bank were interpreted by Oehlert and Swart (2014) as reflecting subaerial exposure during Quaternary low sea-level stands.

Early stage meteoric dissolution and reprecipitation of carbonate may be common in many Holocene and ancient marine and brackish carbonate environments

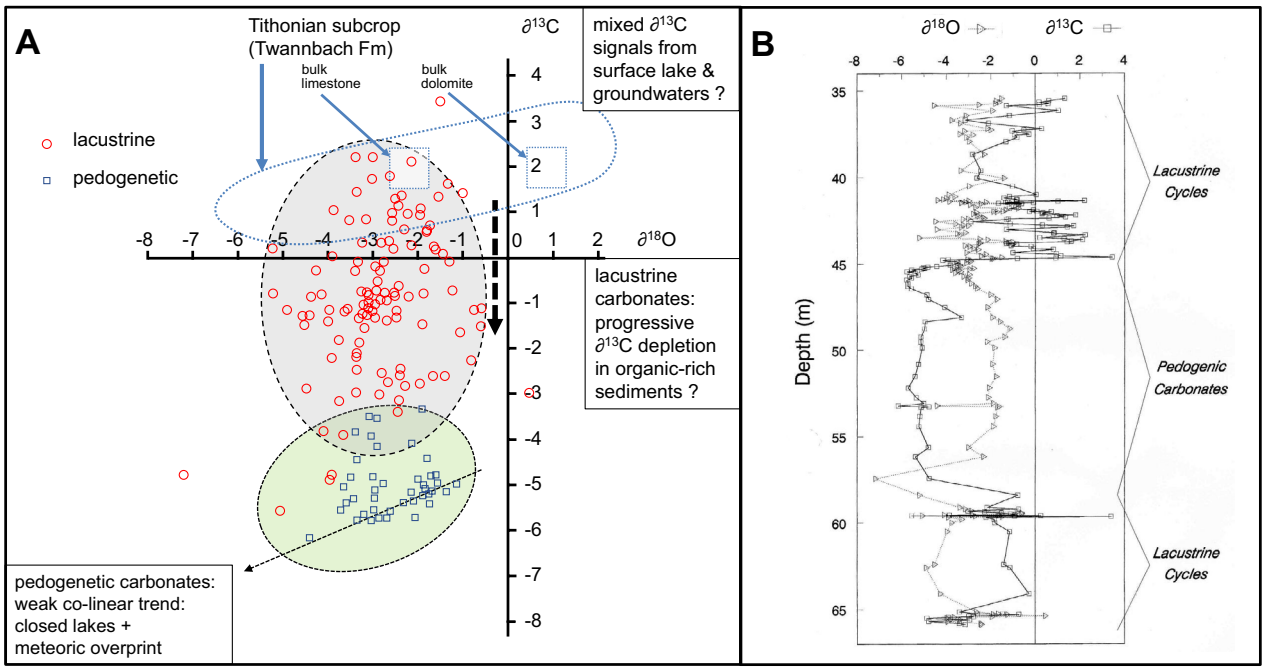


**Fig. 9** Stable isotope data from the Upper Freshwater Molasse: **a** all data, plotting lacustrine/palustrine and pedogenetic carbonates. Data from underlying Tithonian Twannbach Formation marine carbonates from Rameil (2005). **b** Vertical profiles, showing correlation with sedimentary cycles

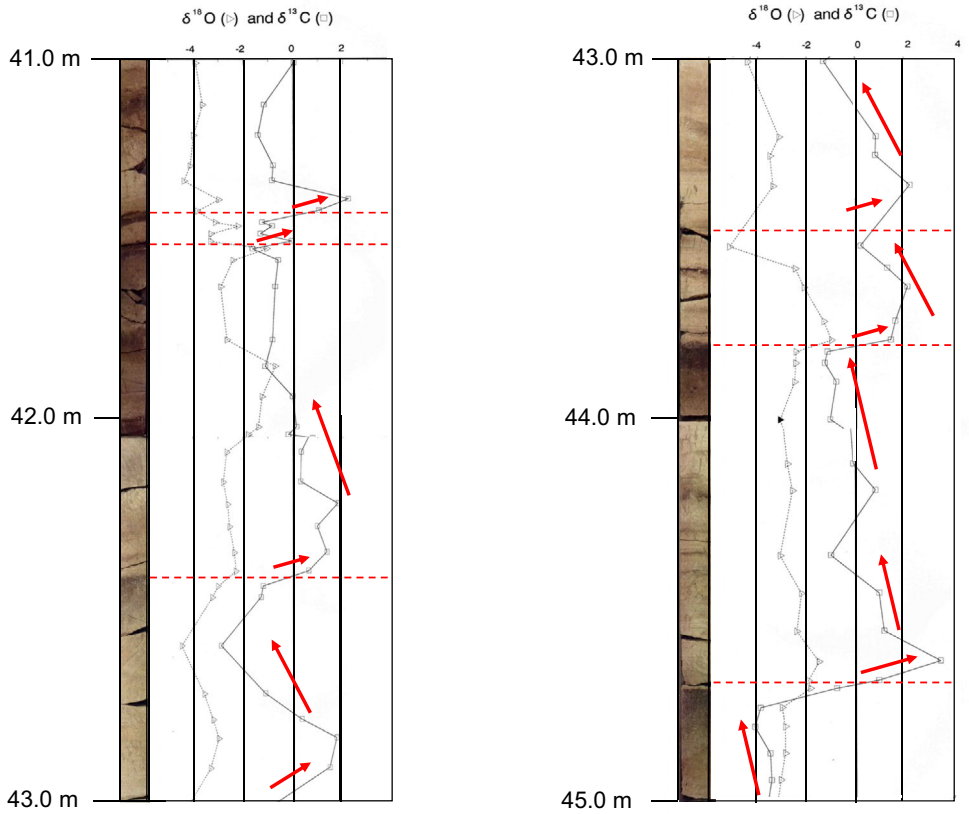


**Fig. 10** Stable isotope data showing typical carbonate sedimentary cycles in lacustrine carbonates from the Upper Freshwater Molasse between 45.0 and 41.0 m. Cycle boundaries shown by red dotted lines, with $\delta^{13}C$ trends shown by red arrows: sharp cycle bases at flooding events with onset of open lacustrine conditions; gradual depletion in $\delta^{13}C$ towards the top of sedimentary cycles associated with increased concentration of $^{13}C$-depleted organic matter

(Mazzullo & Bischoff, 1992; Munnecke et al., 2023; Fetrow et al., 2022; Pederson et al., 2023) and this process can also potentially play a significant role in creating light $\delta^{13}C$ and $\delta^{18}O$ values.

The wider range of $\delta^{13}C$ values shown by the lacustrine facies bears comparison with non-marine carbonates from a range of different settings including the Great Salt Lake, USA (Lindsay et al., 2017) and stream carbonates from the Denizli Graben in SW Turkey (Lopez et al., 2016; de Boever et al., 2017). Study of sediments from Lake Van in SE Turkey also shows how the contribution of different bioclastic and authigenic carbonate phases with diverse stable isotopic signatures can produce a relatively wide scatter of compositions (McCormack & Kwiecien, 2021).

The lacustrine carbonate facies show consistent vertical variations (Fig. 10). Light-coloured carbonate-rich biomicrites at the base of sedimentary cycles, e.g. at 44.7 m, 43.8 m, 41.4 m as shown in Fig. 10, generally show the most positive $^{13}C$ values, passing upwards into darker, more organic-rich limestones displaying more negative $\delta^{18}O$ and markedly more negative $\delta^{13}C$ values.

These vertical variations in $\delta^{13}C$ may reflect cyclical changes in organic productivity. While the lighter-coloured layers may thus record periods of authigenic carbonate sedimentation and extensive $CO_2$ degassing within a hydrologically open system where there was limited burial preservation or post-depositional oxidation of organic material, the dark layers may then reflect final lake filling stages when reduced $CO_2$ degassing and increased deposition of $\delta^{13}C$-depleted organic material led to a progressive depletion in $\delta^{13}C$ towards the tops of each regressive cycle.

The occasional preservation of lamination could also indicate periodic deposition under a stratified water column which served to limit bioturbational mixing and oxidation of organic material while favouring the maintenance of an isotopically light DIC pool. The lighter

sediment layers would then indicate flushing of the system associated with increased groundwater input.

An alternative interpretation could link the observed cyclical variation in $\delta^{13}C$ to increased aquifer discharge during flooding events. While $\delta^{18}O$ values are likely to reflect relatively rapid exchange between lake waters and the atmosphere such that aquifer signal may not be preserved, carbon isotopes may record groundwater influence. Mixing of contrasting dissolved inorganic carbon (DIC) sources from isotopically light surface waters (in equilibrium with terrestrial $C_3$ and aquatic plants) and isotopically heavier groundwaters hosted in underlying marine Jurassic carbonates could thus provide an explanation for the wide range of $\delta^{13}C$ compositions observed. It is interesting that the highest $\delta^{13}C$ values recorded here are similar to those obtained by Rameil (2005) from Twannbach Formation limestones of Tithonian age (Fig. 9) forming the immediate carbonate subcrop in the Tramelan syncline. Nevertheless, there is considerable variability in the stable isotopic composition of Jurassic marine carbonates in the area, with the deeper Reuchenette Formation (Kimmeridgian) showing significantly more negative $\delta^{13}C$ values from +2 to −3 ‰ (Colombie et al., 2011).

## 6 Heavy minerals

### 6.1 Introduction

Early work on the heavy mineral assemblages of the Molasse Basin by Füchtbauer (1964) was followed by detailed outcrop sampling in the eastern Bernese Jura by Hofmann (1969) and Antenen (1973). Later results from Kälin (1993, 1997) were incorporated in a detailed study of heavy minerals from the Palaeogene of the central Jura by Becker (2003). Each of these earlier works demonstrated good correlation between heavy mineral zones and the lithostratigraphy while greatly assisting the understanding of clastic provenance in areas north of the Alps.

Strunck and Matter (2002) provided an overview of heavy mineral distributions in the USM of the western Molasse Basin, while Allen et al., (1985; their Fig. 3) recognised several characteristic heavy mineral assemblages in the OMM, each derived from distinct source areas in the south:

*A southwestern zone* in the western Molasse Basin delivered epidote-apatite-hornblende, with minor clinopyroxenes and serpentine and with pumpellyite decreasing eastwards. This assemblage derives from the western Alps via the Lake Geneva fan (Maurer, 1983);

*A southern zone* in the central Molasse Basin, corresponding to the Napf Fan between Thun and Lucerne, delivered assemblages dominated by epidote; while

Assemblages derived from *an eastern zone* were characterised by apatite and epidote with ultrastable minerals such as zircon and tourmaline, together with staurolite, chloritoid and the characteristic index minerals blue amphibole and lawsonite, and displaying higher garnet contents than in areas to the west. Allen et al. (1985) observed that epidote increases westwards while apatite and ultrastable minerals are more abundant to the east. These diverse assemblages are thought to reflect multiple sediment sources, with the presence of andalusite and topaz at certain horizons suggesting periodic clastic influx from the Bohemian Massif to the east.

### 6.2 Results

The 34 heavy mineral samples from Tramelan-2 show relatively uniform grain sizes throughout (except for the youngest samples and those at 266.3 and 266.0 m). Zircon and tourmaline grain morphologies appear to indicate first cycle derivation, while few of the apatite grains recovered show rounding. Changes in the proportions and the occurrence of key index minerals are therefore likely to reflect provenance rather than environmental effects. Heavy mineral assemblages show distinctive characteristics which differ from the Alpine Molasse as follows:

- *Garnet* is present in only moderate amounts. In the Alpine Molasse of western Switzerland (Strunck, 2001) garnet generally dominates heavy mineral assemblages in the Chattian, while being progressively replaced from the Aquitanian onwards by assemblages containing both apatite and garnet. This observation suggests that the Tramelan-2 succession is likely to be latest Chattian or younger in age;
- Only a single grain of *chrome spinel* was found, despite being generally abundant both in the UMM and as a key mineral in the Chattian USM of eastern and central Switzerland (Gasser, 1968; Schlunegger, et al., 1993, 1997a; Kempf et al., 1999; Strunck, 2001; Schlanke, 2015). Again this is consistent with absence of the lower USM at Tramelan-2.
- *Blue amphibole* is rare, and the associated mineral *lawsonite* is absent in Tramelan-2, contrasting with their characteristic occurrence in heavy mineral suites of Alpine derivation (c.f. Mange-Rajetzky & Oberhänsli, 1982).

- *Pumpellyite* is common in Tramelan-2, as it is from the Burdigalian onwards in the western Molasse Basin, where it likely derives from ophiolites in the Prealps and the schistes lustrés of the Western Alps (Mange-Rajetzky & Oberhänsli, 1986). Pumpellyite is typically much less common than serpentinite elsewhere in the Molasse (Strunck, 2001).
- *Epidote-clinozoisite* is present as very fresh, large crystals in Tramelan-2, in contrast with the smaller and commonly aggregate epidotes found in the Alpine Molasse.
- *Allanite- or piemontite-cored epidotes* were also recovered from Tramelan-2, and these types are also not generally found in the Alpine Molasse.

These observations point to a distinctive sediment provenance history in this part of the Jura. As discussed by Becker (2003) and Berger et al. (2005b), the presence of certain index minerals such as blue hornblende, pumpellyite and serpentine is diagnostic of sediment input from the western Alps delivered by an axial Lake Geneva drainage system (*Genferseeschüttung*), while other more northerly source areas may also have contributed.

### 6.3 Vertical evolution

Four discrete heavy mineral intervals are identified, with the thickest of these divided into two.

### 6.4 Unit 1

274.0–242.0 m. This unit broadly corresponds to the Grey Sandstones described from 275 to 252 m and is provisionally correlated with the fluviatile Upper Alsace Molasse of Roussé (2006). Epidote-clinozoisite is present in moderate amounts, with aggregate forms fairly common. Amphiboles are also important, with blue amphibole in the deepest samples. Apatite occurs in varying quantities, while zircon is sparse and only small amounts of tourmaline are present. Serpentine is rare, except in one sample, and pumpellyite occurs mainly in trace amounts.

#### *6.4.1 Interpretation*

This heavy mineral assemblage appears similar to Strunck's (2001) heavy mineral unit 2 from the Molasse Basin, where the first appearance of hornblende occurs in the USM just below the Chattian/Aquitanian boundary. An alternative assignment to the basal OMM remains feasible.

### 6.5 Unit 2

239.3–162.5 m. This interval can be subdivided into two, both of which show limited numbers of tourmaline, a virtual absence of zircon, and varying, but relatively low quantities of apatite:

a) 239.3–193.3 m. This unit corresponds broadly to the grey sandstones and conglomerates described above from 252 to 190 m. Epidote-clinozoisite is more abundant than in the underlying interval, but many fewer amphiboles are present. Serpentine and pumpellyite are relatively common.
b) 183.6 m–162.5 m. This unit corresponds to the lower section of the Pebbly Sandstones displaying well-developed sedimentary structures. This interval is rich in epidote-clinozoisite and has fairly high proportions of epidote aggregates and very few amphiboles.

#### *6.5.1 Interpretation*

Although the Burdigalian Upper Marine Molasse strata in this interval may rest on a significant discordance representing an appreciable time gap, its association of a high epidote content and the key minerals hornblende and pumpellyite continues to be characteristic of the westerly-derived Lake Geneva system (Becker, 2003).

### 6.6 Unit 3

153.1–112.95 m. This interval corresponds with the upper, more massive section of the Pebbly Sandstones. These strata contain moderate amounts of apatite. Epidote-clinozoisite are abundant but epidote aggregates are rare. Staurolite and tourmaline occur in minor amounts, whilst zircon is virtually absent and amphiboles are rare. Traces of serpentine were found.

The base of mineral suite interval 3 is closely coincident with the occurrence of two key Vêlé Limestone Conglomerate horizons at 154.8 m and at 142 m, while the immediately overlying section between 112.95 m and 104.7 m, approximately 10 m below the interpreted top of the OMM at 95.0 m, shows a decrease in garnet and an increase in epidote and staurolite.

#### *6.6.1 Interpretation*

A switch to epidote-dominated assemblages in the Molasse Basin in the upper part of the OMM was interpreted by Allen et al. (1985) as recording a dilution of westerly-derived index minerals, associated with greater input from the Napf Fan, with transport over a significant distance from the Alps reflecting the assistance of strong tidal currents within a restricted seaway.

### 6.7 Unit 4

104.7–57.1 m. Samples from the marly basal section of the OSM between 57.10 and 91.0 m are highly micaceous with limited quantities of very fine-grained heavy minerals. These strata show the lowest epidote-clinozoisite contents encountered in the Tramelan-2 borehole, with rare epidote aggregates and the highest proportions of apatite. Tourmaline, zircon and staurolite are common. Several amphibole species are present in varying amounts, while serpentine is absent.

#### *6.7.1 Interpretation*

The abundance of mica in this interval and the occurrence of the common ultrastable heavy minerals tourmaline, zircon and staurolite are characteristic of the easterly-derived Micaceous Sandstone drainage system (the *Glimmersandschüttung* of Lemcke et al., 1953; Hofmann, 1969).

## 7 Sedimentological evolution

The basal deposits in Tramelan-2 (275.6–252 m) comprise sandy continental facies similar to those described from the fluviatile Upper Alsace Molasse (USM) of the URG by Roussé (2006), while the overlying OMM succession (252 m–95 m) bears comparison with the OMM of the Molasse Basin to the south (Homewood, 1981; Homewood & Allen, 1981; Allen, 1984; Allen & Homewood, 1984; Keller, 1989, 1990) where many of the same characteristic facies are developed.

The strata from 252 to 190 m appear typical of cyclical shallow water tidal deposits. Conglomeratic lags at cycle bases are interpreted as high energy storm beds recording erosional reworking of the underlying deposits and coarse fluvial input from the hinterland. The bioturbated sands seen above this from 190 to 95 m could be found in a range of shallow marine environments, but in this case are interpreted as subtidal shallow offshore deposits.

The overlying rippled and trough cross-bedded facies record moderate current action, most likely in tidal channels or on the flanks of sand bars. Laminated mudstone-siltstone-sandstone alternations are typical of the upper zones of muddy tidal flats and record deposition from slow-moving currents during slack water phases (Longhitano et al., 2012). Finally, the presence at cycle tops of mottled horizons suggests pedogenetic modification during subaerial exposure, as is commonly seen on the inland margins of tidal flats and salt marshes.

Following early descriptions by Klein (1963) and others, ancient tidal deposits have been described from all around the world (Coughenour et al., 2009). An excellent modern analogue comes from tidal flats inshore of the East Friesian Islands in Germany (Wunderlich, 1969; Reineck & Singh, 1980; Reineck & Wunderlich, 1988). Erosion through tidal channel migration leads to the removal of many of the aeolian and wave-influenced facies of the islands themselves, which show a relatively low preservation potential in comparison with tidal channel facies.

Tidal processes have long been documented from the OMM of the Molasse Basin (Allen & Homewood, 1984) and our work suggests that similar processes acted in the Jura. The OMM in Tramelan-2 is distinctive in showing few wave-generated structures. This is consistent with active tidal channel migration in a meso- or macrotidal, laterally restricted and structurally controlled seaway between the Molasse Basin to the south and the Rhine Graben to the north.

Jost et al. (2016) described wave-influenced facies as limited to the south of the Molasse Basin but not reaching the Jura, consistent with progressive onlap of the OMM to the north. Similarly, Garefalakis and Schlunegger (2019) inferred a wave-dominated coastline with limited tidal influence east of the Napf fan, while a tidal-dominated estuarine environment was developed on the proximal coastal margin to the west, potentially analogous to the setting of Tramelan-2.

High amplitude tides are characteristic of large estuarine systems displaying active tidal channels, sand shoals and broad mud flats. Modern analogues include the Elbe estuary of Germany as above and the Severn estuary of southern England (Allen & Duffy, 1998). Selli et al. (1978) describe how tidal amplification effects in the structurally controlled Messina Strait in southern Italy serve to produce macrotidal conditions within the microtidal Mediterranean.

Continental facies above 95 m are arranged in shallowing upwards sequences recording repeated flooding and infilling episodes. Interbedded marls and limestones from 84 to 66 m reflect ephemeral pond development before an overlying limestone package from 58 to 34 m was laid down in a longer period of lacustrine sedimentation. Seasonal subaerial exposure is inferred by the presence from 55 m to 45 m of palustrine carbonates displaying brecciated and pedogenetic fabrics.

Finally, the dominance of marls with abundant gastropods and peat horizons above 25 m points to the establishment of a freshwater swamp environment in the Tramelan-2 area in association with renewed clastic sedimentation, now including input from basement massifs in the east.

## 8 Stratigraphic development and regional context

### 8.1 Regional onlap

In Cenozoic times, the depocentre and distal pinch-out of each unit in the Molasse was displaced successively northwards ahead of the advancing thrust front and the isostatic load of sediments shed in advance of it (Pfiffner, 1986; Schlunegger et al., 1997c; Pfiffner et al., 2002). Keller (1990, 2012) elegantly interpreted regional stratigraphic variation at the northern margin of the Molasse Basin as reflecting progressive northward onlap and overstep onto the karstified Mesozoic of the European foreland, which itself rests on a top Palaeozoic surface forming a southward dipping regional slope (Rime et al., 2019). This model explains both the northward pinch-out of the USM across the central and eastern Jura (Becker, 2003; Naef et al., 1985: their Fig. 8) and the lateral variation observed in the OMM succession from south to north as discussed above.

At Glovelier, 10 km NE of Tramelan-2 (Fig. 11), Burdigalian strata rest on the marine Jurassic while also thinning northwards as a result of progressive basal onlap. Karst pockets here contain a Burdigalian fauna of MN4 age (Bolliger, 1997; Becker, 2003; Prieto et al., 2018), indicating that the Mesozoic pediment remained exposed into the Miocene or was unroofed by erosion at that time.

Figure 11 presents a regional onlap model, while Figure 12A provides a simplified facies model showing the main environments represented in the OMM at the onset of the Burdigalian transgression, illustrating progressive northward onlap in the Jura and towards basement massifs in the north.

During the Oligocene, freshwater carbonates were deposited in response to karstic discharge in an arc

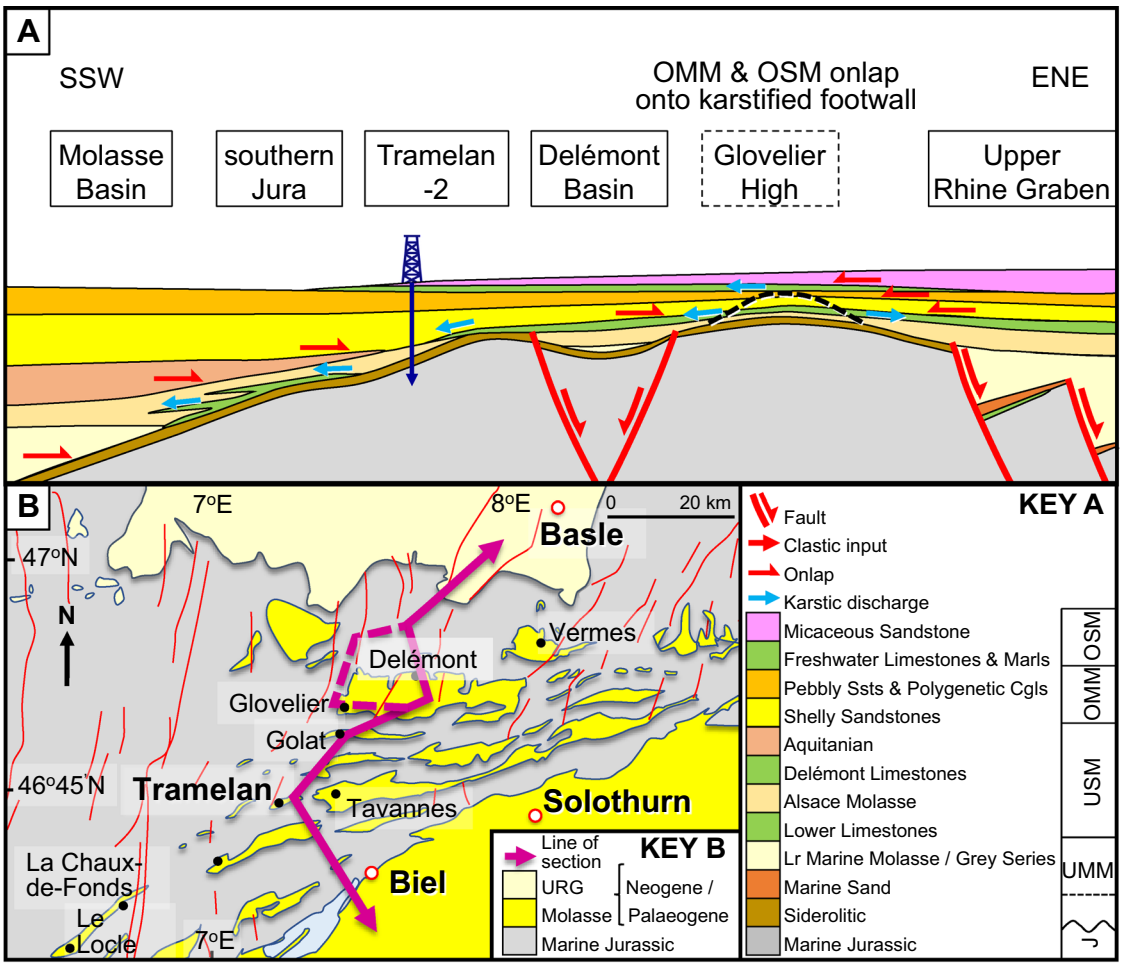


**Fig. 11** Highly schematic section (not to scale) illustrating ENE-ward onlap of the Molasse succession onto the faulted and karstified foreland of the Jura. The dashed section passes over the Glovelier High with additional topographic relief (shown as a dashed line) which was exposed prior to OMM deposition. Intervals of karstic discharge are seen as favouring the deposition of freshwater carbonates at times when topographic relief was infilled and clastic supply was low

30–80 km southwest of Tramelan between Neuchâtel and Lausanne (Platt, 1992), where the USM onlapped the Marine Jurassic and Lower Cretaceous of the southern Jura (Weidmann, 1984). These Chattian Lower Limestones also form a localised veneer on the Mesozoic karst surface in the Jura (Reichenbacher et al., 1996; Becker, 2003; Weidmann et al., 2008).

A similar configuration (Fig. 12B) is thought later to have facilitated renewed deposition of freshwater carbonates in the OSM, through regional onlap onto and karstic discharge from underlying marine Jurassic carbonates in a belt now located further north in the central Jura.

The geological map of Aufranc et al. (2016a) assigns the thin basal Molasse in Tramelan-1 to the USM, as at Tramelan-2, but progressive northward onlap sees the USM absent at Glovelier 10 km to the north, while 3.5 km to WSW of Tramelan-2 in western and southwestern areas of Tramelan village, the Jurassic pediment is overlain directly by younger OSM limestone conglomerates and limestones resting on a basal red marl horizon (Aufranc et al., 2016a; see also Forkert, 1933).

Aufranc et al. (2017) infer from these relationships that the OSM was deposited onto surface relief. This interpretation explains a degree of diachroneity observed within the basal OSM, with a thicker and slightly older section of transitional siltstones and marls resting on the OMM in topographic lows (as at Tramelan-2 and Le Locle), passing upwards into freshwater carbonates which overstep and rest on the karstified Jurassic and a basal conglomerate lag on highs. This onlap geometry would have allowed continued karstic discharge from the Jurassic pediment on highs while the aquifer rose through USM and OMM clastics draping the Mesozoic down slope.

A question then arises whether relief at the base OSM was exclusively erosional, recording the persistence of emergent highs after the OMM transgression, or whether it was partly structurally controlled while reflecting early deformation in the Jura as inferred by Mojon et al. (2018).

### 8.2 Structural controls on Palaeogene–Neogene sedimentation

The structure of the Jura (see Fig. 2) displays a series of en-échelon folds offset by NNE-SSW transverse faults and lateral ramps (Rime et al., 2019). Although the Jura is widely regarded as a predominantly thin-skinned fold-and-thrust belt (Laubscher, 1965, 1987; Sommaruga et al., 2017) compartmentalisation along strike appears to reflect significant pre-existing Variscan structure (Madritsch et al., 2008) which also defines the distribution of underlying Permo-Carboniferous troughs (Diebold & Naef, 1990; Diebold & Noack, 1997).

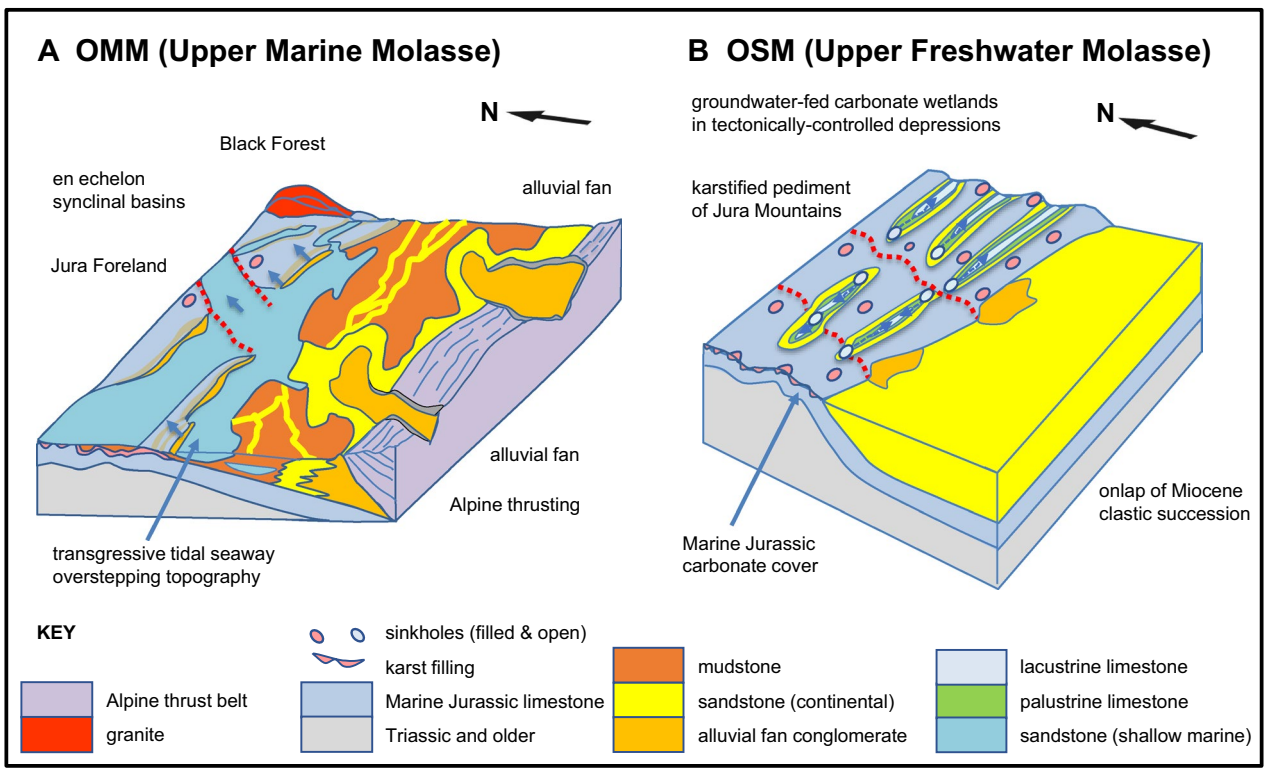


**Fig. 12** Sedimentary facies models. **a** Basal OMM (Upper Marine Molasse). **b** OSM (Upper Freshwater Molasse)

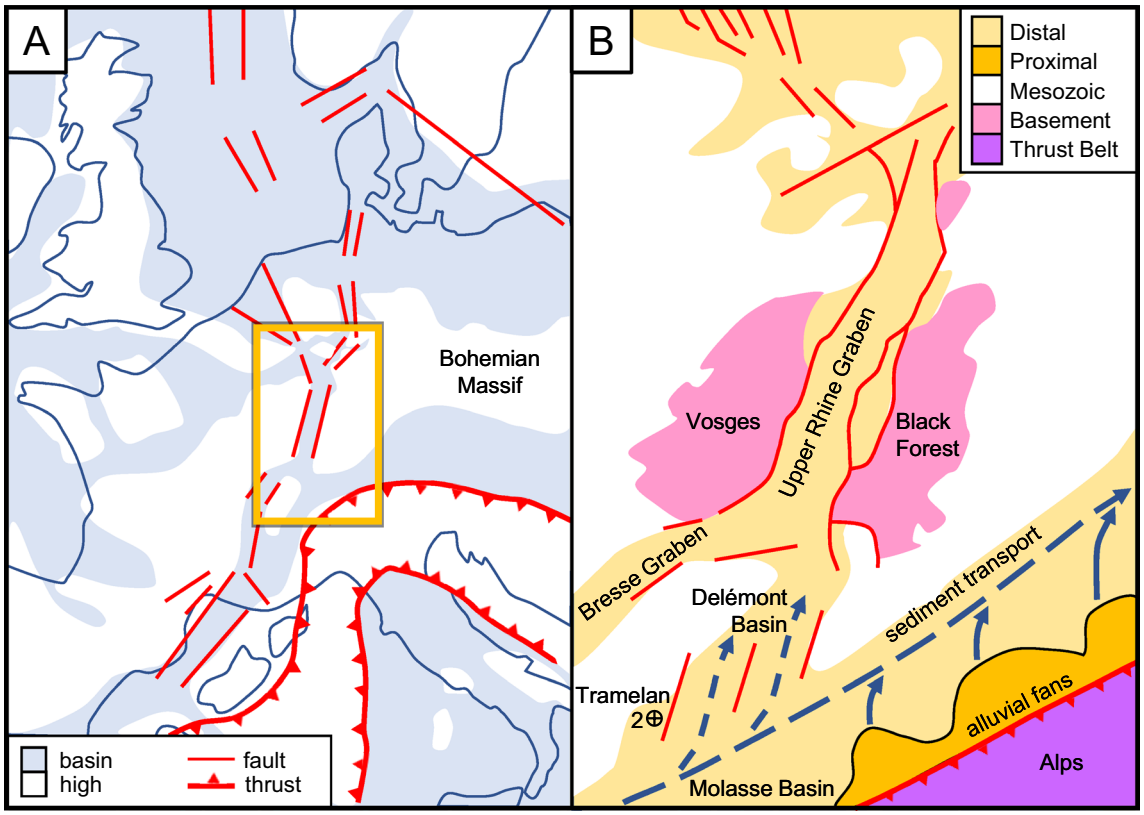


**Fig. 13** **a** Palaeogeographic map of Western Europe in the Upper Rupelian (after Roussé, 2006). The area in **b** is shown in the orange inset box. **b** Schematic palaeogeography of the Molasse Basin and the URG, Early Chattian (Upper Alsace Molasse). Adapted after Pirkenseer et al. (2018)

The same NNE-SSW fault trend defines both the eastern and western margins of the Delémont Basin, with the Glovelier High forming a relatively uplifted footwall block directly to the west. NNE-SSW structures were extensionally reactivated during formation of the URG to the north (Dèzes et al., 2004; Ustaszewski & Schmid, 2006), defining a series of ESE-dipping fault blocks on the northern flanks of the Jura which were passively onlapped by Palaeogene sediments (Hinsken et al., 2007; Ustaszewski et al., 2005) with clastic influx of Chattian Alsace Molasse from the south finally serving to infill this syn-rift relief (Roussé, 2006). With sedimentary gradients then equalised and clastic supply minimised, the Delémont Limestones were laid down as karstic discharge once again flowed onto the surface.

Aquitanian strata seen on the A16 at Tavannes (Zulliger, 2008) are absent at Tramelan-2, where only 1 m of vestigial or reworked Delémont Limestones is preserved. Lateral offset of the Tavannes and Tramelan anticlines suggests that a NNE-SSW transverse fault between them controlled reduced sedimentation or deeper erosion to the west. Karstification of the Glovelier High continued or resumed into the Burdigalian when regional transgression saw OMM deposits onlap pre-existing relief and overstep onto the remaining Jura highs and northern massifs. Formation of a narrow, strongly tidal seaway enabled clastic input from distant source areas in the Alps and from the Vosges and Black Forest. Roussé (2006) and Pirkenseer et al. (2018) envisaged structurally controlled sediment input via the Delémont Basin area (Fig. 13).

Isotopic age dating by Looser et al. (2022) suggested an onset of tectonic activity in the Jura related to Alpine contraction commencing around 14.3 My BP, earlier than determined by biostratigraphy and coinciding with a Middle Miocene (Langhian) age at the latest. This suggests that tectonic enhancement of relief may already have begun by the time of OSM deposition.

Following Langhian sea-level fall, post-rift differential subsidence relief was infilled with basal OSM clastics and marls during renewed transgression, setting the scene for deposition of the overlying Serravallian carbonates as karstic aquifer discharge onto the sediment surface again saw the formation of a groundwater-fed lacustrine-palustrine system. Freshwater carbonate facies development is highly sensitive to tectonically-controlled differential subsidence (Platt & Wright,

1991, 2023), such that a series of small basins with distinct depositional histories and only partial connection may initially have formed along strike (Suter, 1978). However, parallel carbonate facies evolution across a wider area supports the establishment of a common aquifer level within a larger freshwater carbonate system extending SW-NE across the central Jura while connecting at least periodically with depocentres in the URG to the north.

Finally, renewed erosional unroofing of the flanking basement massifs saw clastic sedimentation resume with influx of the Micaceous Sandstones, dated at Tramelan-2 as basal MN7-8 (Kälin, 2001) and derived from the Vosges, Black Forest and Bohemian Massif to the north and east.

## 9 Conclusions

The Tramelan-2 borehole penetrated a 275.60 m thick sequence of sediments from the Lower Freshwater Molasse (USM), Upper Marine Molasse (OMM) and Upper Freshwater Molasse (OSM), presenting a rare continuously cored section through the Cenozoic of the Jura and permitting good correlation with the local and regional lithostratigraphy.

USM continental clastics are sharply overlain by shallow marine clastics of the OMM, passing upwards into non-marine clastics and carbonates in the OSM above. The succession displays distinctive heavy mineral assemblages reflecting derivation from a range of sources in the western Alps, from the Napf Fan, as well as from northerly non-Alpine source terranes.

Sedimentological facies analysis of the OMM in the Tramelan-2 borehole reveals a series of stacked shallow marine regressive cycles, each lying on a sharply-defined transgressive base.

Indications of strong current action and limited evidence for wave influence point to sedimentation in a protected meso- or macrotidal flat or estuarine complex within a structurally controlled narrow seaway between the Molasse Basin in the south and the URG in the north.

Later regression and erosion is thought to have resulted in rejuvenation of a regional karst system developed in the Mesozoic carbonate pediment. Carbonates and marls in the overlying Upper Freshwater Molasse onlapped and overstepped onto erosional and potentially early tectonic relief, while reflecting deposition in freshwater carbonate swamps, marshes and lakes. Repeated shallowing upward cycles capped by organic-rich calcareous peat record successive phases of lake infilling. The middle part of the succession comprises palustrine carbonates, which were periodicially modified by pedogenesis when lower aquifer levels resulted in seasonal or longer intervals of subaerial exposure.

Stable isotopic compositions of the freshwater carbonates reflect the influence of pedogenesis during subaerial exposure of palustrine facies. Cyclical variations in $\delta^{13}C$ may reflect changes in lake productivity associated with the progressively increasing incorporation of $^{13}C$-depleted organic matter towards the top of lake-filling cycles. An alternative interpretation could nevertheless correlate positive $\delta^{13}C$ excursions during episodic flooding events with increased aquifer discharge of groundwaters in equilibrium with underlying marine Jurassic carbonates.

## Supplementary Information

The online version contains supplementary material available at https://doi.org/10.1186/s00015-023-00436-1.

**Additional file 1.** Core photographs from the Tramelan-2 borehole.

**Acknowledgements**
We thank Mr. J.-P. Clément for borehole access and the late Dr. J.-P. Berger for palaeontological determinations. We are grateful to Prof. Stephen Burns for stable isotope analyses and to the late Dr Maria Mange-Rajetzky for heavy mineral analyses. Mr. Andy Werthemann took core photos and Mr Vlado Greco prepared thin sections. We thank Dr. Beat Keller for discussions on the Molasse, Dr. Chelsea Pederson and Dr. Anne Fetrow for helpful review of stable isotope results and Dr. Damien Becker for kindly sharing unpublished regional correlations as shown in Fig. 4. Reviews by Drs. Daniel Kälin and Claudius Pirkenseer improved the manuscript significantly.

**Notes**
For convenience we have used the German abbreviations UMM, OMM, and USM, OSM for the Lower and Upper Marine, and Lower and Upper Freshwater Molasse, respectively.

**Author contributions**
AM provided the research facilities and oversaw the study while co-ordinating access to the borehole site and core, and reviewing the heavy mineral results and regional interpretations. NHP carried out sedimentological analysis and interpretations and produced the article.

**Funding**
The work was carried out under a Swiss National Science Foundation grant.

**Data availability**
Core samples were stored at the Institut für Geologie of the Universität Bern. Heavy mineral analyses and palaeontological specimens are unfortunately no longer available due to the sad demise of Drs. Mange-Rajetsky and Berger.

## Declarations

**Ethics approval and consent to participate**
Not applicable.

**Consent for publication**
Not applicable.

**Competing interests**
The authors have no conflicts of interest to declare.

**Author details**
[1]Institut für Geologie, Universität Bern, Baltzerstrasse 1-3, 3012 Bern, Switzerland. [2]Present Address: Energean UK Ltd., 44 Baker Street, London W1U 7AL, UK.

Received: 21 July 2022 Accepted: 24 May 2023
Published online: 28 July 2023

**References**

Allen, P. A. (1984). Reconstruction of ancient sea conditions with an example from the Swiss Molasse. *Marine Geology., 60*, 455–473. https://doi.org/10.1016/0025-3227(84)90162-2

Allen, J. R. L., & Duffy, M. J. (1998). Temporal and spatial depositional patterns in the Severn Estuary, southwestern Britain; intertidal studies at spring-neap and seasonal scales, 1991–1993. *Marine Geology, 146*, 147–171. https://doi.org/10.1016/S0025-3227(97)00124-2

Allen, P. A., & Homewood, P. (1984). Evolution and mechanics of a Miocene tidal sandwave. *Sedimentology, 31*, 63–81. https://doi.org/10.1111/j.1365-3091.1984.tb00723.x

Allen, P. A., Mange-Rajetzky, M., Matter, A., & Homewood, P. (1985). Dynamic palaeogeography of the open Burdigalian seaway, Swiss Molasse Basin. *Eclogae geologicae Helvetiae, 78*, 351–381. https://doi.org/10.5169/SEALS-165661

Alonso Zarza, A. (2003). Palaeoenvironmental significance of palustrine carbonates and calcretes in the geological record. *Earth Science Reviews, 60*, 261–298. https://doi.org/10.1016/S0012-8252(02)00106-X

Antenen, M. A. (1973). Geologie der Montoz-Kette unter besonderer Berücksichtigung des Tertiärs in den angrenzenden Mulden von Péry und Tavannes. Inauguraldissertation der Philosophisch-naturwissenschaftlichen Fakultät der Universität Bern. 167 p. Universität Bern. https://slsp-ube.primo.exlibrisgroup.com/discovery/fulldisplay?docid=alma991166802447055 11&context=L&vid=41SLSP_UBE:UBE&lang=en

Armenteros, I. Daley, B., & García, E., (1997). Lacustrine and palustrine facies in the Bembridge Limestone (late Eocene, Hampshire Basin) of the Isle of Wight, southern England. *Palaeogeography, Palaeoclimatology, Palaeoecology, 128*, 111–132. https://doi.org/10.1016/S0031-0182(96)00108-3

Aufranc, J., Jordan, P., Piquerez, A., Hofman, B., Andres, B., & Burkhalter, R. (2017). Atlas géologique de la Suisse 1:25'000, feuille 1125 Chasseral, notice explicative 155 (pp. 1–160 plus annexes) Wabern: Office fédéral de topographie swisstopo, Wabern, Switzerland. https://shop.swisstopo.admin.ch/en/maps/geological-maps/explanatory-booklet-geological-atlas-switzerland-25000#collapse-node-174

Aufranc, J., Jordan, P., Piquerez, A., Kälin, D., & Burkhalter, R. (2016a). Atlas géologique de la Suisse 1:25'000, feuille 1105 Bellelay, avec partie est de la feuille 1104 Saignelégier, notice explicative 147 (pp. 1–140). Office fédéral de topographie swisstopo, Wabern, Switzerland. https://shop.swisstopo.admin.ch/en/maps/geological-maps/explanatory-booklet-geological-atlas-switzerland-25000#collapse-node-166

Aufranc, J., Laubscher, H. P., Suter, M., & Burkhalter, R. (2016b). Atlas géologique de la Suisse 1:25'000, feuille 1105 Bellelay, avec partie est de la feuille 1104 Saignelégier. Wabern: Office fédéral de topographie swisstopo, Wabern, Switzerland. https://shop.swisstopo.admin.ch/en/maps/geological-maps/explanatory-booklet-geological-atlas-switzerland-25000#collapse-node-166

Azerêdo, A. C., Wright, V. P., Mendonça-Filho, J., Cabral, M. C., & Duarte, L. V. (2015). Deciphering the history of hydrologic and climatic changes on carbonate lowstand surfaces: Calcrete and organic-matter/evaporite facies association on a palimpsest Middle Jurassic landscape from Portugal. *Sedimentary Geology, 323*, 66–91. https://doi.org/10.1016/j.sedgeo.2015.04.12

Baumberger, E. (1923). Die Bohnerze im Delsberger Becken. In: Die Eisen- und Manganerze der Schweiz. *Beiträge zur Geologie der Schweiz, (Geotechnische Serie), 13*, 77–125. https://shop.swisstopo.admin.ch/de/node/516/download

Baumberger, E. (1927). Die stampischen Bildungen der Nordschweiz und ihrer Nachbargebiete mit besonderer Berücksichtigung der Mollusken-faunen. *Eclogae geologicae Helvetiae, 20*, 533–578. https://www.e-periodica.ch/digbib/view?pid=egh-001%3A1926%3A20%3A%3A559

Beaumont, G., de Chambrier, A., & Weidmann, M. (1984). Présence d'*Eucricetodon* (Rodentia) dans la Molasse marine du synclinal de Tavannes (Jura bernois). *Bullétin de la Société Vaudoise des Sciences Naturelles, 365*, 73–78. https://www.worldcat.org/title/presence-deucricetodon-rodentia-dans-la-molasse-marine-du-synclinal-de-tavannes-jura-bernois/oclc/603736328

Becker, D. (2003). Paléoécologie et paléoclimats de la Molasse du Jura (Oligo-Miocène): apport des Rhinoceratoidea (Mammalia) et des minéraux argileux. Thèse Univ Fribourg, *Geofocus, 9*, 1–327. https://doc.rero.ch/record/4478/files/BeckerD.pdf

Becker, D., Picot, L., & Berger, J.-P. (2001b). Stable isotopes ($\delta^{13}C$, $\delta^{18}O$) on charophyte gyrogonites: Results from the Brochene Fluh section (Oligo-Miocene boundary, Swiss Molasse). *Geobios, 35*, 89–97. https://doi.org/10.1016/S0016-6995(02)00012-8

Becker, D., Rössner, G. E., Picot, L., & Berger, J.-P. (2001a). Early Miocene ruminants from Wallenried (USM, Aquitanian/Switzerland): biostratigraphy and paleoecology. *Eclogae geologicae Helvetiae, 94*, 547–564. https://www.e-periodica.ch/digbib/view?pid=egh-001%3A2001%3A94%3A%3A575

Berger, J.-P. (2011). Du Bassin molassique au fossé rhénan: évolution des paléoenvironnements dans un avant pays dynamique. *Géochronique, 117*, 47–49. https://scholar.google.com/scholar_lookup?journal=G%C3%A9ochroniques,+Magazine+des+G%C3%A9osciences&title=Du+bassin+molassique+au+foss%C3%A9+rh%C3%A9nan,+%C3%A9volution+des+pal%C3%A9oenvironnements+dans+un+avant+pays+dynamique&author=J-P+Berger&volume=117&publication_year=2011&pages=44-49&

Berger, J.-P., Reichenbacher, B., Becker, D., Grimm, M., Grimm, K., Picot, L., Storni, A., Pirkenseer, C., & Schäfer, A. (2005a). Eocene-Pliocene time scale and stratigraphy of the Upper Rhine Graben (URG) and the Swiss Molasse Basin (SMB). *International Journal of Earth Sciences, 94*, 711–731. https://doi.org/10.1007/s00531-005-0479-y

Berger, J.-P., Reichenbacher, B., Becker, D., Grimm, M., Grimm, K., Picot, L., Storni, A., Pirkenseer, C., & Schäfer, A. (2005b). Paleogeography of the Upper Rhine Graben (URG) and the Swiss Molasse Basin (SMB) from Eocene to Pliocene. *International Journal of Earth Sciences, 94*, 697–710. https://doi.org/10.1007/s00531-005-0475-2

Bertrand, J. (1990). Données pour la protection et la gestion de l'eau souterraine du canton de Bern. Région de Tramelan. Campagne de sondages profonds (1988). Direction des transports, de l'énergie et des eaux du canton de Berne (DTEE), 43p. https://www.bvd.be.ch/content/dam/bvd/dokumente/fr/awa/umwelt/geologie/grundlagenberichte-region-jura/r%C3%A9gion-de-tramelan-campagne-de-sondages-profonds-de.pdf

Bolliger, T. (1997). Advantages and disadvantages of the scientific use of karst faunas. In: Aguilar, J. P., Legendre, S., & Michaux, J. (Editors), Actes du Congres BiochroM' 1997. *Mémoires et travaux de l'Institut de Montpellier de l'Ecole Pratique Hautes Etudes, 21*, 39–45. https://www.researchgate.net/profile/Thomas-Bolliger/publication/268872094_Advantage_and_disadvantage_of_the_scientific_use_of_karstic_faunas/links/547a299f0cf205d1687fac82/Advantage-and-disadvantage-of-the-scientific-use-of-karstic-faunas.pdf

Burkhard, M., & Sommaruga, A. (1980). Evolution of the western Swiss Molasse basin: Structural relations with the Alps and the Jura belt. In: Mascle, A., Puigdefàbregas, C., Luterbacher, H. P., & Fernàndez, M., (Editors), *Cenozoic Foreland Basins of Western Europe. Special Publication of the Geological Society of London, 134*, 279–298. https://doi.org/10.1144/GSL.SP.1998.134.01.13

Bustillo, M. A., & Alonso-Zarza, A. M. (2007). Overlapping of pedogenesis and meteoric diagenesis in distal alluvial and shallow lacustrine deposits in the Madrid Miocene Basin, Spain. *Sedimentary Geology, 198*, 255–271. https://doi.org/10.1016/j.sedgeo.2006.12.006

Cerling, T. E. (1984). The stable isotopic composition of modern soil carbonate and its relationship to climate. *Earth and Planetary Science Letters, 71*, 229–240. https://doi.org/10.1016/0012-821X(84)90089-X

Cerling, T. E. (1991). Carbon dioxide in the atmosphere: Evidence from Cenozoic and Mesozoic paleosols. *American Journal of Science, 291*, 377–400. https://doi.org/10.2475/ajs.291.4.377

Cerling, T. E., Quade, J., Yang, Y., & Bowman, J. R. (1989). Carbon isotopes in soils and paleosols as ecology and paleoecology indicators. *Nature, 341*, 138–139. https://doi.org/10.1038/341138a0

Chauve, P., Enay, R., Fluck, P., & Sittler, C. (1980). L'Est de la France (Vosges, Fossé Rhénan, Bresse, Jura). *Annales Scientifiques de l'Université de Besançon, 4*, 3–80. https://scholar.google.com/scholar_lookup?title=L%E2%80%99Est%20de%20la%20France%20%28Vosges%2C%20Foss%C3%A9%20Rh%C3%A9nan%2C%20Bresse%2C%20Jura%29&journal=Annales%20scientifiques%20de%20l%E2%80%99Universit%C3%A9%20de%20Besan%C3%A7on&volume=4&issue=1&pages=3-80&publication_year=1980&author=Chauve%2CP&author=Enay%2CR&author=Fluck%2CP

Clément, I., & Berger, J.-P. (1999). Nouvelles données stratigraphiques sur la Molasse du bassin de Delémont et du synclinal de Foradrai (Oligo-Miocene, Jura Suisse). *Neues Jahrbuch für Geologie und Paläontologie Abhandlungen, 214*, 463–485. https://doi.org/10.1127/njgpa/214/1999/463

Cohen, K. M., Harper, D. A. T., Gibbard, P. L., & Fan, J. -X. (2022). ICS International Chronostratigraphic Chart 2022/03. International Commission on Stratigraphy, IUGS. Retrieved July 14, 2022 from https://stratigraphy.org/ICSchart/ChronostratChart2020-03.pdf

Colombie, C., Lécuyer, C., & Strasser, A. (2011). Carbon- and oxygen-isotope records of palaeoenvironmental and carbonate production changes in shallow-marine carbonates (Kimmeridgian, Swiss Jura). *Geological Magazine, 148*, 133–153. https://doi.org/10.1017/S0016756810000518

Coughenour, C. L., Archer, A. W., & Lacovara, K. J. (2009). Tides, tidalites, and secular changes in the Earth-Moon system. *Earth-Science Reviews, 97*, 59–79. https://doi.org/10.1016/j.earscirev.2009.09.002

de Boever, E., Brasier, A. T., Foubert, A., & Kele, S. (2017). What do we really know about early diagenesis of non-marine carbonates? *Sedimentary Geology, 361*, 25–51. https://doi.org/10.1016/j.sedgeo.2017.09.011

de Klein, G. V. (1963). Bay of Fundy intertidal zone sediments. *Journal of Sedimentary Petrology, 33*, 844–854. https://doi.org/10.1306/74D70F5B-2B21-11D7-8648000102C1865D

de Klein, G. V. (1975a). Tidalites in the Eureka Quartzite (Ordovician), Eastern California and Nevada. In R. N. Ginsburg (Ed.), *Tidal Deposits* (pp. 45–153). Springer Verlag. https://doi.org/10.1007/978-3-642-88494-8_17

de Klein, G. V. (1975b). Paleotidal range sequences, middle member, Wood Canyon Formation (Late Precambrian), Eastern California and Western Nevada. In R. N. Ginsburg (Ed.), *Tidal Deposits* (pp. 171–178). Springer Verlag. https://doi.org/10.1007/978-3-642-88494-8_20

de Raaf, J. F. M., & Boersma, J. R. (2007). Tidal deposits and their sedimentary structures (Seven examples from Western Europe). *Geologie en Mijnbouw, 50*, 479–504. https://dspace.library.uu.nl/handle/1874/28547

Dean, W. E., & Fouch, T. D. (1983). Lacustrine environment. In: Scholle, P. A., Bebout, D. G., & Moore, C. H., (Editors), *Carbonate Depositional Environments. Memoir of the American Association of Petroleum Geologists*, *33*, 96-130. https://doi.org/10.1306/M33429C6

Dèzes, P., Schmid, S. M., & Ziegler, P. A. (2004). Evolution of the European Cenozoic rift system: interaction of the Alpine and Pyrenean orogens with their foreland lithosphere. *Tectonophysics, 389*, 1–33. https://doi.org/10.1016/j.tecto.2004.06.011

Diebold, P., & Noack, T. (1997). Late Palaeozoic troughs and Tertiary structures in the eastern Folded Jura. *Deep Structure of the Swiss Alps. Results of NRP, 20*, 59–63. https://scholar.google.com/scholar?q=Late%20Paleozoic%20troughs%20and%20Tertiary%20structures%20in%20the%20eastern%20folded%20Jura&author=P.%20Diebold&author=T.%20Noack&author=O.A.%20Pfiffner&publication_year=1997&journal=Deep%20Structure%20of%20the%20Swiss%20Alps%E2%80%93Results%20From%20NRP%2020&volume=20&pages=59-63

Diebold, P., & Naef, H. (1990). Der Nordschweizer Permokarbontrog. *Nagra Informiert, 2*, 29–36. http://scholar.google.com/scholar_lookup?&title=Der%20Nordschweizer%20Permokarbontrog&journal=Nagra%20informiert&volume=2&issue=1990&pages=29-36&publication_year=1990&author=Diebold%2CP&author=Naef%2CH

Dunagan, S. P., & Turner, C. E. (2004). Regional paleohydrologic and paleoclimatic settings of wetland/lacustrine depositional systems in the Morrison Formation (Upper Jurassic), Western Interior, USA. *Sedimentary Geology, 167*, 269–296. https://doi.org/10.1016/j.sedgeo.2004.01.007

Dustin, N. M., Wilkinson, B. H., & Owen, R. M. (1986). Littlefield Lake, Michigan: Carbonate budget of Holocene sedimentation in a temperate-region lacustrine system. *Limnology and Oceanography, 31*, 1301–1311. https://doi.org/10.4319/Lo.1986.31.6.1301

Eichenberger, U., Mojon, P.-O., Gogniat, S., Pictet, A., Blant, D., Locatelli, D., Metral, V., & Morard, A. (2020). Atlas géologique de la Suisse 1:25'000, feuille 1143 Le Locle, avec partie de feuille 1123 Le Russey, notice explicative 172 (pp. 1–176 plus annexe). Office fédéral de topographie swisstopo, Wabern. https://shop.swisstopo.admin.ch/en/maps/geological-maps/explanatory-booklet-geological-atlas-switzerland-25000#collapse-node-187

Fetrow, A. C., Snell, K. E., Di Fiori, R. V., Long, S. P., & Bonde, J. W. (2022). How hot is too hot? Disentangling Mid-Cretaceous hothouse paleoclimate from diagenesis. *Paleoceanography and Paleoclimatology, 37*, e2022PA004517. https://doi.org/10.1029/2022PA004517

Forkert, E. (1933). Geologische Beschreibung des Kartengebietes Tramelan im Berner Jura. *Eclogae geologicae Helvetiae, 26*, 1–41. https://www.e-periodica.ch/digbib/view?pid=egh-001%3A1933%3A26%3A%3A10#20

Frei, E. (1925). Zur Geologie des südöstlichen Neuenburger Juras insbesondere des Gebietes zwischen Gorges de l'Areuse und Gorges du Seyon. *Beiträge zur Geologischen Karte der Schweiz N.F. 55*(1),1–98. https://scholar.google.com/scholar?cluster=6434674241347577479&hl=en&as_sdt=2005&sciodt=0,5&as_ylo=2015

Füchtbauer, H. (1964). Sedimentpetrographische Untersuchungen in der älteren Molasse nördlich der Alpen. *Eclogae geologicae Helvetiae, 57*, 157–298. https://www.e-periodica.ch/digbib/view?pid=egh-001%3A1964%3A57%3A%3A12#262

Garefalakis, P., & Schlunegger, F. (2019). Tectonic processes, variations in sediment flux, and eustatic sea level recorded by the 20 Myr old Burdigalian transgression in the Swiss Molasse basin. *Solid Earth, 10*, 2045–2072. https://doi.org/10.5194/se-10-1-2019

Gasser, U. (1968). Die innere Zone der subalpinen Molasse des Entlebuchs (Kt. Luzern): Geologie und Sedimentologie. *Eclogae geologicae Helvetiae, 61*, 229–319. https://www.e-periodica.ch/digbib/view?pid=egh-001%3A1968%3A61%3A%3A252

Glass, S. W., & Wilkinson, B. H. (1980). The Peterson limestone—early cretaceous lacustrine carbonate deposition in western Wyoming and southeastern Idaho. *Sedimentary Geology, 27*, 143–160. https://doi.org/10.1016/0037-0738(80)90034-2

Heim, A. (1919). Geologie der Schweiz. Band I: Molasseland und Juragebirge. Tauchnitz, Leipzig. 704p. https://scholar.google.com/scholar?cluster=5138739338365649473&hl=en&as_sdt=2005&sciodt=0,5

Hinsken, S., Ustaszewski, K., & Wetzel, A. (2007). Graben width controlling syn-rift sedimentation: The Palaeogene southern Upper Rhine Graben as an example. *International Journal of Earth Sciences (Geologische Rundschau), 96*, 979–1002. https://doi.org/10.1007/s00531-006-0162-y

Hofmann, F. (1969). Neue Befunde über die westliche Fortsetzung des beckenaxialen Glimmersand-Stromsystems in der Oberen Süsswassermolasse des schweizerischen Alpenvorlandes. *Eclogae geologicae Helvetiae, 61*, 279–284. https://doi.org/10.5169/seals-163701

Hofmann, F., Reichenbacher, B., & Farley, K. A. (2017). Evidence for >5 Ma paleoexposure of an Eocene-Miocene paleosol of the Bohnerz Formation, Switzerland. *Earth and Planetary Science Letters, 465*, 168–175. https://doi.org/10.1016/j.epsl.2017.02.042

Homewood, P., Allen, P. A., & Williams, G. D. (1986). Dynamics of the Molasse Basin of western Switzerland. In P. A. Allen & P. Homewood (Eds.), *Foreland Basins. Special Publication of the International Association of Sedimentologists, 8,* (pp. 199–219). Blackwell Scientific Publications. https://doi.org/10.1002/9781444303810.ch10

Homewood, P. (1981). Faciès et environnements de dépôt de la Molasse de Fribourg. *Eclogae geologicae Helvetiae, 74*, 29–36. https://doi.org/10.5169/seals-165088

Homewood, P., & Allen, P. A. (1981). Wave-, tide- and current-controlled sandbodies of Miocene Molasse, western Switzerland. *Bulletin of the American Association of Petroleum Geologists, 65*, 2534–2545. https://doi.org/10.1306/03B599FE-16D1-11D7-8645000102C1865D

Hug, W. A., Berger ,J-P., Clément,I., Käin, D., & Weidmann, M. (1997). Miocene fossiliferous paleokarst (MN 4) and OSM deposits (MN5- ?) near Glovelier (Swiss Jura Mountains). Meeting of Molasse Group, 24, January 1997 in Fribourg, Abstracts: 16–17. https://scholar.google.com/scholar?hl=en&as_sdt=0%2C5&q=Miocene+fossiliferous+paleokarst+%28MN+4%29+and+OSM+deposits+%28MN5-+%3F%29+near+Glovelier+%28Swiss+Jura+Mountains%29.+&btnG=

Jost, J., Kempf, O., & Kälin, D. (2016). Stratigraphy and palaeoecology of the Upper Marine Molasse (OMM) of the central Swiss Plateau.

*Swiss Journal of Geosciences, 109*, 149–169. https://doi.org/10.1007/s00015-016-0223-6

Kälin, D. (1993). Stratigraphie und Säugerfaunen der Oberen Süsswassermolasse der Nordwestschweiz. Unpublished PhD Thesis, No. 10152, Eidgenössische Technische Hochschule, Zürich. https://doi.org/10.3929/ethz-a-000904767

Kälin, D. (1997). Litho- und Biostratigraphie der mittel- bis obermiocänen Bois de Raube-Formation (Nordwestschweiz). *Eclogae geologicae Helvetiae, 90*, 97–114. https://www.e-periodica.ch/digbib/view?pid=egh-001%3A1997%3A90%3A%3A119

Kälin, D. (2001). Paléontologie et âge de la molasse d'eau douce supérieure (OSM) du Jura neuchâtelois. *Mémoires Suisses de Paléontologie, 121*, 65–99. https://doc.rero.ch/record/210205/files/PAL_E4305.pdf

Kälin, D., & Kempf, O. (2009). High-resolution mammal biostratigraphy in the Middle Miocene continental record of Switzerland (Upper freshwater Molasse, MN 4 – MN 9, 17 – 10 Ma) : part I : part II. Report OAI. https://doc.rero.ch/record/13668

Kälin, D., Weidmann, M., Engesser, B., & Berger, J.-P. (2001). Paléontologie et âge de la Molasse d'eau douce supérieure (OSM) du Jura neuchâtelois. *Mémoires Suisses de Paléontologie, 121*, 65–99. http://data.rero.ch/01-R007763585

Keller, B. (1989). Fazies und Stratigraphie der Oberen Meeresmolasse (unteres Miozän) zwischen Napf und Bodensee. Inauguraldissertation der Philosophisch-naturwissenschaftlichen Fakultät der Universität Bern. 307 p. Universität Bern. https://unige.swisscovery.slsp.ch/discovery/fulldisplay?docid=alma991000228999705502&context=L&vid=41SLSP_UGE:VU1&lang=fr&search_scope=MyInst_and_CI&adaptor=Local%20Search%20Engine&tab=41SLSP_UGE_MyInst_CI&query=any,contains,keller%20fazies%20molasse

Keller, B. (1990). Wirkung von Wellen und Gezeiten bei der Ablagerung der Oberen Meeresmolasse. Löwendenkmal und Gletschergarten – zwei anschauliche geologische Studienobjekte. *Mitteilungen der Naturforschenden Gesellschaft Luzern*, *31*, 245–271. https://doi.org/10.5169/seals-523687

Keller, B. (1992). Hydrogeologie des schweizerischen Molasse-Beckens: Aktueller Wissensstand und weiterführende Betrachtungen. *Eclogae geologicae Helvetiae, 85*, 611–651. https://www.e-periodica.ch/digbib/view?pid=egh-001%3A1992%3A85%3A%3A531#641

Keller, B. (2012). Facies of Molasse based on a section across the central part of the Swiss Plateau. *Swiss Bulletin für Angewandte Geologie, 17* (2), 3–19. https://doi.org/10.5169/seals-349238

Kelts, K., & Talbot, M. (1990). Lacustrine carbonates as geochemical archives of environmental change and biotic/abiotic interactions. In M. M. Tilzer & L. Serruya (Eds.), *Large lakes: Ecological structure and function* (pp. 288–315). Springer-Verlag. https://doi.org/10.1007/978-3-642-84077-7_15

Kempf, O., Matter, A., Burbank, D. W., & Mange, M. (1999). Depositional and structural evolution of a foreland basin margin in a magnetostratigraphic framework: The Eastern Swiss Molasse Basin. *International Journal of Earth Sciences, 88*, 253–275. https://doi.org/10.1007/s005310050263

Kübler, B. (1962). Etude de l'Oehningien (Tortonien) du Locle (Neuchâtel-Suisse). *Bulletin de la Société Neuchâteloise des Sciences Naturelles, 85*, 1–42. https://www.e-periodica.ch/digbib/view?pid=bsn-002%3A1962%3A85#11

Kuhlemann, J., & Kempf, O. (2002). Post-Eocene evolution of the North Alpine Foreland Basin and its response to Alpine tectonics. *Sedimentary Geology, 152*, 45–78. https://doi.org/10.1016/S0037-0738(01)00285-8

Laubscher, H. P. (1965). Ein kinematisches Modell der Jurafaltung. *Eclogae geologicae Helvetiae, 58*, 231–318. https://www.e-periodica.ch/digbib/view?pid=egh-001%3A1965%3A58%3A%3A5#246

Laubscher, H. P. (1977). Fold development in the Jura. *Tectonophysics, 37*, 337–362. https://doi.org/10.1016/0040-1951(77)90056-7

Laubscher, H. P. (1981). The 3D propagation of décollement in the Jura. In: McClay, K. R. & Price, N. J. (Editors), *Thrust and Nappe Tectonics*. *Special Publication of the Geological Society of London, 9*, 311–317. https://doi.org/10.1144/GSL.SP.1981.009.01.27

Laubscher, H. P. (1987). Die tektonische Entwicklung der Nordschweiz. *Eclogae geologicae Helvetiae, 80*, 287–303. https://doi.org/10.5169/seals-165996

Laubscher, H. P. (1992). Jura kinematics and the Molasse Basin. *Eclogae geologicae Helvetiae, 85*, 653–675. https://doi.org/10.5169/seals-167024

Lemcke, K., Engelhardt, V., & Füchtbauer, H. (1953). Geologische und sedimentpetrographische Untersuchungen im Westteil der ungefalteten Molasse des süddeutschen Alpenvorlandes. *Beihefte zum Geologischen Jahrbuch. 11*, 1–64. https://www.schweizerbart.de/publications/detail/isbn/9783510968299/Beih_11_z_Geol_Jahrb

Lindsay, M. R., Anderson, C., Fox, N., Scofield, G., Allen, J., Anderson, E., Bueter, L., Poudel, S., Sutherland, K., Munson-McGee, J. H., Van Nostrand, D., Zhou, J., Spear, J. R., Baxter, R. K., Lageson, D. R., & Boyd, E. S. (2017). Microbialite response to an anthropogenic salinity gradient in Great Salt Lake, Utah. *Geobiology, 15*, 131–145. https://doi.org/10.1111/gbi.12201

Liniger, H. (1925). Geologie des Delsberger Beckens und der Umgebung von Movelier. *Beiträge zur Geologischen Karte der Schweiz, N.F. 55,* 1–71. https://unige.swisscovery.slsp.ch/discovery/fulldisplay?docid=alma991005260989705502&context=L&vid=41SLSP_UGE:VU1&lang=fr&search_scope=MyInst_and_CI&adaptor=Local%20Search%20Engine&tab=41SLSP_UGE_MyInst_CI&query=sub,exact,Del%C3%A9mont,AND&mode=advanced

Longhitano, S. G., Mellere, D., Steel, R. J., & Ainsworth, R. B. (2012). Tidal depositional systems in the rock record: A review and new insights. *Sedimentary Geology, 279*, 2–22. https://doi.org/10.1016/j.sedgeo.2012.03.024

Looser, N., Madritsch, H., Guillong, M., Laurent, O., Wohlwend, S., & Bernasconi, S. M. (2021). Absolute age and temperature constraints on deformation along the basal décollement of the Jura fold-and-thrust belt from carbonate U-Pb dating and clumped isotopes. *Tectonics, 40*, e2020TC006439. https://doi.org/10.1029/2020TC006439

Lopez, B., Camoin, G., Özkul, M., Swennen, R., & Virgone, A. (2016). Sedimentology of coexisting travertine and tufa deposits in a mounded geothermal spring carbonate system, Obruktepe, Turkey. *Sedimentology, 64*, 903–931. https://doi.org/10.1111/sed.12284

Madritsch, H., Schmid, S. M., & Fabbri, O. (2008). Interactions between thin- and thick-skinned tectonics at the northwestern front of the Jura fold-and-thrust belt (eastern France). *Tectonics, 27*, 2008TC002282. https://doi.org/10.1029/2008TC002282

Mange-Rajetzky, M. A., & Oberhänsli, R. (1982). Detrital lawsonite and blue sodic amphibole in the Molasse of Savoy, France and their significance in assessing Alpine evolution. *Schweizerische Mineralogische und Petrologische Mitteilungen*, *62*, 415–436. http://pascal-francis.inist.fr/vibad/index.php?action=getRecordDetail&idt=PASCALGEODEBRGM8320328198

Mange-Rajetzky, M. A., & Oberhänsli, R. (1986). Detrital pumpellyite in the peri-Alpine molasse. *Journal of Sedimentary Research, 56*, 112–122. https://doi.org/10.1306/212F889B-2B24-11D7-8648000102C1865D

Mas, R., Arribas, E., González-Acebrón, L., Quijada, E., & Campos-Soto, S. (2019). Coastal wetlands as markers of transgression in proximal extensional systems (Berriasian, W Cameros Basin, Spain). *Journal of Iberian Geology, 45*, 1–27. https://doi.org/10.1007/s41513-018-0086-y

Matter, A., Homewood, P. Caron, C., Rigassi, D., van Stuijvenberg, J., Weidmann, M,& Winkler, W. (1980). Flysch and Molasse of Western and Central Switzerland. Excursion No. 126A of the 26th International Geological Congress. In: Trümpy, R. (Editor), *Geology of Switzerland, a Guide-Book. Part B: Geological Excursions*, 261–293. https://boris.unibe.ch/id/eprint/90903

Matter, A., & Weidmann, M. (1992). Tertiary sedimentation in the Swiss Molasse: An overview. Symposium Swiss Molasse Basin. *Eclogae geologicae Helvetiae, 85*, 776–777. https://doi.org/10.5169/seals-167041

Maurer, H. (1983). Sedimentpetrographische Analysen an Molasseabfolgen der Westschweiz. *Jahrbuch der Geologischen Bundesanstalt, Wien, 126*, 23–69. https://opac.geologie.ac.at/ais312/dokumente/JB1261_023_A.pdf

Mazzullo, S. J., & Bischoff, W. D. (1992). Meteoric calcitization and incipient lithification of recent high-magnesium calcite muds, Belize. *Journal of Sedimentary Research, 62*(2), 196–207. https://doi.org/10.1306/D42678C0-2B26-11D7-8648000102C1865D

McCormack, J., & Kwiecien, O. (2021). Coeval primary and diagenetic carbonates in lacustrine sediments challenge palaeoclimate interpretations. *Scientific Reports, 11*, 7935. https://doi.org/10.1038/s41598-021-86872-1

Mojon, P.-O., de Känel, E., Kälin, D., Becker, D., Pirkenseer, C. M., Rauber, G., Ramseyer, K., Hostettler, B., & Weidman, M. (2018). New data on the biostratigraphy (charophytes, nannofossils, mammals) and lithostratigraphy of the Late Eocene to Early Late Miocene deposits in the Swiss

Molasse Basin and Jura Mountains. *Swiss Journal of Palaeontology, 137*, 1–48. https://doi.org/10.1007/s13358-017-0145-6
Munnecke, A., Wright, V. P., & Nohl, T. (2023). The origins and transformation of carbonate mud during early marine burial diagenesis and the fate of aragonite: a stratigraphic sedimentological perspective. *Earth Science Reviews, 239*, 104366. https://doi.org/10.1016/j.earscirev.2023.104366
Murphy, D. H., & Wilkinson, B. H. (1980). Carbonate deposition and facies distribution in a central Michigan marl lake. *Sedimentology, 27*, 123–135. https://doi.org/10.1111/j.1365-3091.1980.tb01164.x
Naef, H., Diebold, P., & Schlanke, S. (1985). Sedimentation und Tektonik im Tertiär der Nordschweiz. Nagra Technischer Bericht, NTB 85–14. Nagra, Baden. https://www.nagra.ch/en/technischer-bericht-85-14
Oehlert, A., & Swart, P. (2014). Interpreting carbonate and organic carbon isotope covariance in the sedimentary record. *Nature Communications, 5*, 4672. https://doi.org/10.1038/ncomms5672
Pederson, C. L., Klaus, J. S., McNeill, D. F., & Swart, P. K. (2023). Freshwater microbial mud: Punctuated diagenesis during marine transgression in the Florida Everglades. *Sedimentology* (submitted).
Pederson, C. L., Klaus, J. S., Swart, P. K., & McNeill, D. F. (2019). Deposition and early diagenesis of microbial lime mud in the Florida Everglades. *Sedimentology, 66*, 1989–2010. https://doi.org/10.1111/sed.12569
Pfiffner, O. A. (1986). Evolution of the north Alpine foreland basin in the central Alps. In: Allen, P. A., & Homewood, P. (Editors), *Foreland Basins. Special Publication of the International Association of Sedimentologists, 8*, 219–228. https://doi.org/10.1002/9781444303810.ch11
Pfiffner, O. A., Schlunegger, F., & Buiter, S. J. H. (2002). The Swiss Alps and their peripheral foreland basin: Stratigraphic response to deep crustal processes. *Tectonics, 21*, 1009. https://doi.org/10.1029/2000TC900039
Picot, L. (2002). Le Paléogène des synclinaux du Jura et de la bordure sud-rhénane : paléontologie (Ostracodes), paléoécologie, biostratigraphie et paléogéographie. Thèse Univ. Fribourg, *Geofocus*, *5*, pp 1–240. https://folia.unifr.ch/unifr/documents/299782
Picot, L., Becker, D., & Berger, J.-P. (1999). Nouvelles données paléoécologiques et biostratigraphiques sur la Formation des Calcaires delémontiens ("Delsberger Kalke", Oligocène terminal, Jura Suisse). *Neues Jahrbuch für Geologie und Paläontologie Abhandlungen, 214*, 433–462. https://doi.org/10.1127/njgpa/214/1999/433
Pirkenseer, C., Rauber, G., & Roussé, S. (2018). A revised Palaeogene lithostratigraphic framework for the Northern Swiss Jura and the southern Upper Rhine Graben and its relationship to the North Alpine Foreland Basin. *Rivista Italiana di Paleontología e Stratigrafía, 124*, 163–246. https://doi.org/10.13130/2039-4942/9867
Platt, N. H. (1989). Lacustrine carbonates and pedogenesis: Sedimentology and origin of palustrine deposits from the Early Cretaceous Rupelo Formation, W Cameros Basin, N Spain. *Sedimentology, 36*, 665–684. https://doi.org/10.1111/j.1365-3091.1989.tb02092.x
Platt, N. H. (1992). Fresh-water carbonates from the Lower Freshwater Molasse (Oligocene, western Switzerland): Sedimentology and stable isotopes. *Sedimentary Geology, 78*, 81–99. https://doi.org/10.1016/0037-0738(92)90114-7
Platt, N. H., (1995) Sedimentation and tectonics of a syn-rift succession: Upper Jurassic alluvial fans and palaeokarst at the late Cimmerian unconformity, Western Cameros Basin, northern Spain. In: Plint, G. (Editor), *Sedimentary Facies Analysis. Special Publication of the International Association of Sedimentologists, 22*, 219–236. https://doi.org/10.1002/9781444304091.ch9
Platt, N. H., & Keller, B. (1992). Distal alluvial deposits in a foreland basin setting: The Lower Freshwater Molasse (Lower Miocene), Switzerland: Sedimentology, architecture and palaeosols. *Sedimentology, 39*, 545–565. https://doi.org/10.1111/j.1365-3091.1992.tb02136.x
Platt, N. H., & Wright, V. P. (1991). Lacustrine carbonates: facies models, facies distributions and hydrocarbon aspects. In: Anadón, P, Cabrera, Ll. & Kelts, K. (Editors), *Lacustrine Facies Analysis. Special Publication of the International Journal of Sedimentologists, 13*, 57–74. https://doi.org/10.1002/9781444303919.ch3
Platt, N. H., & Wright, V. P. (1992). Palustrine carbonates and the Florida Everglades: Towards an exposure index for the fresh-water environment? *Journal of Sedimentary Petrology, 62*, 1058–1071. https://doi.org/10.1306/D4267A4B-2B26-11D7-8648000102C1865D
Platt, N. H., & Wright, V. P. (2019). The flooding of a carbonate platform: The eastern Yucatán Platform as a model for transgressive carbonates. *Search and Discovery*, 51600. http://www.searchanddiscovery.com/documents/2019/51600wright/ndx_wright.pdf / https://doi.org/10.1306/51600Platt2019
Platt, N. H., & Wright, V. P. (2023). Flooding of a carbonate platform: The Sian Ka'an Wetlands, Yucatán, Mexico – a model for the formation and evolution of palustrine carbonate factories around the modern Caribbean Sea and in the depositional record. *The Depositional Record, 9*, 99–151. https://doi.org/10.1002/dep2.217
Prieto, J., Becker, D., Rauber, G., & Pirkenseer, C. M. (2018). New biostratigraphical data for the Burdigalian Montchaibeux Member at the locality Courrendlin-Solé (Canton of Jura, Switzerland). *Swiss Journal of Geosciences, 111*, 1–11. https://doi.org/10.1007/s00015-017-0285-0
Rameil, N. (2005). Carbonate sedimentology, sequence stratigraphy, and cyclostratigraphy of the Tithonian in the Swiss and French Jura Mountains: a high-resolution record of changes in sea level and climate. Thèse de doctorat: Université de Fribourg, 245p. *Geofocus*, *13*. https://folia.unifr.ch/unifr/documents/300025
Reichenbacher, B., Berger, J.-P., & Weidmann, M. (1996). Charophytes et otolithes de la Molasse d'eau douce inférieure de Moutier (Jura Suisse). *Neues Jahrbuch für Geologie und Paläontologie Abhandlungen, 202*, 63–93. https://doi.org/10.1127/njgpa/202/1996/63
Reichenbacher, B., Krijgsman, W., Lataster, Y., Pippèr, M., Van Baak, C. G. C., Chang, L., Kälin, D., Jost, J., Doppler, G., Jung, D., Prieto, J., Abdul Aziz, H., Bôhme, M., Garnish, J., Kirscher, U., & Bachtadse, V. (2013). A new magnetostratigraphic framework for the Lower Miocene (Burdigalian/Ottnangian, Karpatian) in the North Alpine Foreland Basin. *Swiss Journal of Geosciences, 106*, 309–334. https://doi.org/10.1007/s00015-013-0142-8
Reineck, H.-E., & Singh, I. B. (1980). *Depositional Sedimentary Environments* (2nd ed., p. 549). Springer Verlag. https://doi.org/10.1007/978-3-642-81498-3
Reineck, H.-E., & Wunderlich, F. (1988). Lamination and laminated rhythmites in water-laid sands. *Senckenbergiana Maritima, 28*, 227–235. https://doi.org/10.1007/BF03043151
Riding, R. (1979). Origin and diagenesis of lacustrine algal bioherms at the margin of the Ries crater, Upper Miocene, southern Germany. *Sedimentology, 26*, 645–680. https://doi.org/10.1111/j.1365-3091.1979.tb00936.x
Rime, V., Sommaruga, A., Schori, M., & Mosar, J. (2019). Tectonics of the Neuchâtel Jura Mountains: Insights from mapping and forward modelling. *Swiss Journal of Geosciences, 112*, 563–578. https://doi.org/10.1007/s00015-019-00349-y
Rollier, L. (1892). Étude stratigraphique sur les terrains tertiaires du Jura bernois (partie méridionale). Dix coupes du Tertiaire jurassien. *Eclogae geologicae Helvetiae, 3*, 43–84. https://www.e-periodica.ch/digbib/view?pid=egh-001%3A1892%3A3%3A%3A65#55
Rollier, L. (1893). Étude stratigraphique sur les terrains Tertiaires du Jura Bernois (Partie septentrionale): Nouvelles coupes du Tertiare Jurassien. *Eclogae geologicae Helvetiae, 4*, 1–27. https://www.e-periodica.ch/digbib/view?pid=egh-001%3A1893%3A4%3A%3A5
Rollier, L. (1900). Carte téctonique des environs de Bellelay (Jura bernois) 1:25'000. Schweizerische Geologische Kommission. http://viaf.org/viaf/45058352
Rollier, L. (1910). Nouvelles observations sur le Sidérolithique et la Molasse oligocène du Jura central et septentrional. Troisième supplément à la description géologique de la partie jurassienne de la feuille VII de la carte géologique de la Suisse au 1:100'000. *Matériaux pour la carte géologique de la Suisse, (N.S.), 25*, 1–148. https://www.e-periodica.ch/digbib/view?pid=egh-001%3A1892%3A3%3A%3A65#55
Rollier, L. (1898). 2e supplément à la description géologique de la partie jurassienne de la feuille VII de la carte géologique de la Suisse 1: 100'000. *Matériaux pour la carte géologique de la Suisse, (N.S.), 8*, 1–206. https://scholar.google.com/scholar_lookup?title=Troisi%C3%A8me%20suppl%C3%A9ment%20%C3%A0%20la%20description%20g%C3%A9ologique%20de%20la%20partie%20jurassienne%20de%20la%20feuille%20VII%20de%20la%20carte%20g%C3%A9ologique%20de%20la%20Suisse%20au%201%3A%20100%20000.%20Premi%C3%A8re%20partie%3A%20Nouvelles%20observations%20sur%20le%20Sid%C3%A9rolithique%20et%20la%20Molasse%20oligoc%C3%A8ne%20du%20Jura%20central%20et%20m%C3%A9ridional&journal=Mat%C3%A9riaux%20pour%20la%20Carte%20G%C3%A9ologique%20de%20la%20Suisse&volume=25&publication_year=1910&author=Rollier%2CL

Rothpletz, W. (1933). Geologische Beschreibung der Umgebung von Tavannes im Berner Jura. *Verhandlungen der Naturforschenden Gesellschaft in Basel, 43*, 12–150. https://bib.rero.ch/global/documents/729528

Roussé, S. (2006). Architecture et dynamique des séries marines et continentales de l'oligocène moyen et supérieur du sud du fossé rhénan: Evolution des milieux de dépôt en contexte de rift en marge de l'avant-pays alpin. Thèse de doctorat en Sciences de l'Univers. Sédimentologie, Université Louis Pasteur, Strasbourg. 474 pp. https://publication-theses.unistra.fr/public/theses_doctorat/2006/ROUSSE_Stephane_2006.pdf

Schlaich, E. (1934). Geologisches Beschreibung der Gegend von Court im Berner Jura. *Eclogae geologicae Helvetiae, 26*, 1–41. https://www.e-periodica.ch/digbib/view?pid=egh-001%3A1933%3A26%3A%3A10#20

Schlanke, S. (2015). Sedimentpetrographische und tektonische Gliederung der Molasse in der Bohrung St. Gallen GT-1. *Berichte der St. Gallischen Naturwissenschaftlichen Gesellschaft, 99*, 393–410. https://www.e-periodica.ch/digbib/view?pid=sgn-005%3A2015%3A93%3A%3A397

Schlunegger, F., Jordan, T. E., & Klappa, E. M. (1997c). Controls of erosional denudation in the orogen on foreland basin evolution: The Oligocene central Swiss Molasse Basin as an example. *Tectonics, 16*, 823–840. https://doi.org/10.1029/97TC01657

Schlunegger, F., Leu, W., & Matter, A. (1997b). Sedimentary sequences, seismic facies, subsidence analysis, and evolution of the Burdigalian Upper Marine Molasse Group, Central Switzerland. *Bulletin of the American Association of Petroleum Geologists, 81*, 1185–1207. https://doi.org/10.1306/522B4A19-1727-11D7-8645000102C1865D

Schlunegger, F., Matter, A., & Mange, M. A. (1993). Alluvial fan sedimentation and structure of the southern Molasse Basin margin, Lake Thun area, Switzerland. *Eclogae geologicae Helvetiae, 86*, 717–750. https://www.e-periodica.ch/digbib/view?pid=egh-001%3A1993%3A86%3A%3A752

Schlunegger, F., Matter, A., Burbank, D. W., & Klaper, E. M. (1997a). Magnetostratigraphic constraints on relationships between evolution of the central Swiss Molasse Basin and Alpine orogenic events. *Bulletin of the Geological Society of America*, *109*, 225–241. https://doi.org/10.1130/0016-7606(1997)109%3c0225:MCORBE%3e2.3.CO;2

Schori, M., Zwaan, F., Schreurs, G., & Mosar, J. (2021). Pre-existing basement faults controlling deformation in the Jura Mountains fold-and-thrust belt: insights from analogue models. *Tectonics, 814*, 228980. https://doi.org/10.1016/j.tecto.2021.228980

Selli, R., Colantoni, P., Fabbri, A., Rossi, S., Borsetti, A. M., & Gallignani, P. (1978). Marine geological investigation on the Messina Strait and its approaches. *Giornale di Geologia, 42*, 1–70. http://pascal-francis.inist.fr/vibad/index.php?action=getRecordDetail&idt=9496798

Sissingh, W. (1998). Comparative Tertiary stratigraphy of the Rhine Graben, Bresse Graben and Molasse Basin: Correlation of Alpine foreland events. *Tectonophysics, 300*, 249–284. https://doi.org/10.1016/S0040-1951(98)00243-1

Sommaruga, A. (1996). Geology of the central Jura and the Molasse basin: new insight into an evaporite-based foreland fold and thrust belt (Doctoral dissertation, Université de Neuchâtel). 176 pp.. https://libra.unine.ch/handle/123456789/19422

Sommaruga, A., Mosar, J., Schori, M., & Gruber, M. (2017). The Role of the Triassic evaporites underneath the north Alpine foreland. In: Soto, J. I., Flinch, J. F., & Tari, G., (Editors), *Permo-Triassic Salt Provinces of Europe, North Africa and the Atlantic Margins*, pp. 447–466. Elsevier Inc.. https://doi.org/10.1016/b978-0-12-809417-4.00021-5

Spicher, A. (1980). Tektonische Karte der Schweiz: 1: 500 000. Bern: Schweizerische Geologische Kommission. https://opendata.swiss/dataset/tektonische-karte-der-schweiz-1-500000

Stankevica, K., Vincevica-Gaile, Z., & Klavins, M. (2016). Freshwater sapropel (gyttja): its description, properties and opportunities of use in contemporary agriculture. *Agronomy Research, 14*, 929–947. https://agronomy.emu.ee/wp-content/uploads/2016/05/Vol14-_nr3_Stankevica.pdf#abstract-4337

Strunck, P. (2001). The Molasse of Western Switzerland. Unpublished PhD thesis, University of Bern, 146 pp. https://www.worldcat.org/title/molasse-of-western-switzerland/oclc/83518051

Strunck, P., & Matter, A. (2002). Depositional evolution of the western Swiss Molasse. *Eclogae geologicae Helvetiae, 95*, 197–222. https://www.e-periodica.ch/digbib/view?pid=egh-001%3A2002%3A95%3A%3A3#213

Suter, M. (1978). Geologische Intepretation eines reflexionsseismischen W-E-Profils durch das Delsberger Becken (Faltenjura). *Eclogae geologicae Helvetiae, 71*, 267–275. https://www.e-periodica.ch/digbib/view?pid=egh-001%3A1978%3A71%3A%3A288

Talbot, M. R. (1990). A review of the palaeohydrological interpretation of carbon and oxygen isotopic ratios in primary lacustrine carbonates. *Chemical Geology (Isotope Geoscience Section), 80*, 261–179. https://doi.org/10.1016/0168-9622(90)90009-2

Treese, K. L., & Wilkinson, B. H. (1982). Peat-marl deposition in a Holocene paludal-lacustrine basin – Sucker Lake, Michigan. *Sedimentology, 29*, 375–390. https://doi.org/10.1111/j.1365-3091.1982.tb01801.x

Trümpy, R. (1980). *Geology of Switzerland, a Guide-Book. Part A: An Outline of the Geology of Switzerland*. Wepf. & Co., Basel. ISBN: 3859770624 9783859770621 3859770632 9783859770638. https://pascal-francis.inist.fr/vibad/index.php?action=getRecordDetail&idt=PASCALGEODEBRGM8120326514

Tütken, T., Vennemann, T. W., Janz, H., & Heizmann, E. P. J. (2006). Palaeoenvironment and palaeoclimate of the Middle Miocene lake in the Steinheim basin, SW Germany: A reconstruction from C, O, and Sr isotopes of fossil remains. *Palaeogeography, Palaeoclimatology, Palaeoecology, 241*, 457–491. https://doi.org/10.1016/j.palaeo.2006.04.007

Ustaszewski, K., & Schmid, S. M. (2006). Control of preexisting faults on geometry and kinematics in the northernmost part of the Jura fold-and-thrust belt. *Tectonics, 25*, 2005TC001915. https://doi.org/10.1029/2005TC001915

Ustaszewski, K., Schumacher, M. E., & Schmid, S. M. (2005). Simultaneous normal faulting and extensional flexuring during rifting: An example from the southernmost Upper Rhine Graben. *International Journal of Earth Sciences (Geologische Rundschau), 94*, 680–696. https://doi.org/10.1007/s00531-004-0454-z

Weidmann, M. (1984). Le Sidérolithique et la molasse basale d'Orbe (VD). *Bulletin de la Société Vaudoise des Sciences Naturelles, 77*, 135–141. https://doi.org/10.5169/seals-278507

Weidmann, M., Berger, J.-P., Engesser, B., Reichenbacher, B., Sauvagnat, J., & Schäfer, P. (2008). La Molasse de la Vallée de Joux (Jura, Suisse et France). *Bullétin de la Sociéte Vaudoise des Sciences Naturelles, 91*, 69–101. https://doi.org/10.5169/seals-278507

Wright, V. P., & Platt, N. H. (1995). Seasonal wetland carbonate sequences and dynamic catenas: A re-appraisal of palustrine limestones. *Sedimentary Geology, 99*, 65–71. https://doi.org/10.1016/0037-0738(95)00080-R

Wunderlich, F. (1969). Studien zur Sedimentbewegung, Transportformen und Schichtbildung im Gebiet der Jade. *Senckenbergiana Maritima, 1(50)*, 107–146. https://scholar.google.com/scholar_lookup?title=Studien%20zur%20Sedimentbewegung.%20I.%20Transportformen%20und%20Schichtbildung%20im%20Gebiet%20der%20Jade&journal=Senckenbergiana%20marit.&volume=50&issue=1&pages=107-146&publication_year=1969&author=Wunderlich%2CF.

Ziegler, P. (1956). Geologische Beschreibung des Blattes Courtelary (Berner Jura) und zur Stratigraphie des Séquanien im zentralen Schweizer Jura. Beiträge zur Geologischen Karte der Schweiz N.F.F., *102*, 1–101. https://scholar.google.com/scholar?hl=en&as_sdt=0%2C5&q=ziegler+Geologische+Beschreibung+des+Blattes+Courtelary+%28Berner+Jura%29+und+zur+Stratigraphie+des+S%C3%A9quanien+im+zentralen+Schweizer+Jura&btnG=

Ziegler, P., & Fraefel, M. (2009). Response of drainage systems to Neogene evolution of the Jura fold-thrust belt and Upper Rhine Graben. *Swiss Journal of Geosciences, 102*, 57–75. https://doi.org/10.1007/s00015-009-1306-4

Zulliger, L. (2008). Etude lithostratigraphique et paléontologique de la molasse de Tavannes (Jura bernois): accompagné d'une compilation cartographique des remplissages Cénozoïques du Jura central. Mémoire de master: Bibliothèque cantonale jurassienne, 87 pp. Available from https://core.ac.uk/download/pdf/20663107.pdf

## Publisher's Note